




Oral administration of a whole glucan particle (WGP)-based therapeutic cancer vaccine targeting macrophages inhibits tumor growth

Liuyang He^{1,2} · Yu Bai² · Lei Xia² · Jie Pan² · Xiao Sun² · Zhichao Zhu² · Jun Ding² · Chunjian Qi²  · Cui Tang¹

Received: 29 June 2021 / Accepted: 20 December 2021 / Published online: 4 January 2022
© The Author(s), under exclusive licence to Springer-Verlag GmbH Germany, part of Springer Nature 2022

Abstract

Although therapeutic cancer vaccines have been gaining substantial ground, the development of cancer vaccines is impeded because of the undegradability of delivery systems, ineffective delivery of tumor antigens and weak immunogenicity of adjuvants. Here, we made use of a whole glucan particle (WGP) to encapsulate ovalbumin (OVA), thereby formulating a novel cancer vaccine. Results from in vitro experiments showed that WGP-OVA not only induced the activation of bone marrow-derived macrophages (BMDMs) including driving M0 BMDM polarization to the M1 phenotype, upregulating the costimulatory molecules and inducing the generation of cytokines, but also facilitated antigen presentation. After oral administration of the WGP-OVA formulation to mice with OVA-expressing tumors, these particles can increase tumor-infiltrating OVA-specific CD8⁺ CTLs and repolarize tumor-associated macrophages (TAMs) toward M1-like phenotype, which led to delayed tumor progression. These findings revealed that WGP could serve as both an antigen delivery system and an adjuvant system for promising cancer vaccines.

Keywords Whole glucan particle (WGP) · Cancer vaccine · Macrophages · Oral administration

Introduction

Antigen-specific cancer vaccines, aiming to exploit the powers of the patients' own immune system to destroy cancer cells, have attracted the attention of medical researchers and serve as effective tools in cancer immunotherapy. Generally, cancer vaccines consist of tumor antigens (including peptides, proteins and DNA or mRNA encoding antigens) that are specifically expressed on tumor cells, targeted carriers capable of protecting antigens from degradation and transporting antigens into antigen-presenting cells (APCs), and vaccine adjuvants that function as immunopotentiators [1].

Despite considerable progress in developing tumor vaccines, challenges such as the ineffective delivery of antigens and weak immunogenicity and toxicity of carriers remain barriers to their wide clinical translation [2]. Thus, it is urgent to search for more suitable carriers with low toxicity and adjuvants capable of enhancing antigen immunogenicity to increase the translation relevance of the antigen-based cancer vaccine platform.

β -Glucan, a naturally occurring polysaccharide, is commonly located in cell walls of plants, fungi and algae. The biological activity of β -glucan including anti-tumor and anti-infective effects has been extensively investigated, which is dependent on varied source and structure [3, 4]. Researches proved that only yeast-derived β -glucans, which possess β -1,3-D-glucan backbone grafted with long β -1,6-glucan side chains, behave as immunomodulators [5]. The immune function of yeast-derived β -glucans is mainly attributed to β -1,3-D-glycoside, a ligand of the dectin-1 receptor, through which β -glucans can be recognized and endocytosed by immune cells expressing Dectin-1, such as macrophages and DCs [6]. Herein, an insoluble β -glucan particle derived from the cell walls of *Saccharomyces cerevisiae* (whole glucan particle, WGP) was used

✉ Chunjian Qi
qichunjian@njmu.edu.cn

✉ Cui Tang
tangcui@fudan.edu.cn

¹ State Key Laboratory of Genetic Engineering, Department of Pharmaceutical Science, School of Life Science, Fudan University, Shanghai 200433, China

² Medical Research Center, The Affiliated Changzhou No. 2 People's Hospital of Nanjing Medical University, Changzhou 213003, China

as an adjuvant carrier for cancer vaccines. These hollow particles with 2–4 μm in diameter maintain an intact yeast cellular structure and are mainly composed of long-chain β -1,3-glucans that form a triple-helix structure with pores over the whole surface [7]. Based on the above-mentioned structure properties, WGP has been previously reported to serve as a delivery system for encapsulation with proteins (including antigens) [8, 9], DNA [10], and siRNA [11, 12]. Once such particulate β -glucan attaches the extracellular C-type lectin domain of Dectin-1, the intracellular ITAM (immunoreceptor tyrosine-based activation motif)-like motif (hemITAM) is phosphorylated for the initiation of the hemITAM signaling pathway, which causes a series of inflammatory responses such as phagocytosis, oxidative burst, cytokine/chemokine production and antigen presentation [13]. Therefore, WGP appears to be the desirable candidate for use both as a carrier loading antigen and as an adjustment of the tumor vaccine in terms of its specific structure and immunomodulatory properties [14].

The immunomodulatory function of WGP is affected by routes of administration. Recently, more researchers have focused on the mechanism underlying the immune activation induced by oral administration of WGP and found that oral administration is an effective route by which the WGP enters the bloodstream to exert its biological activity [15]. Owing to the lack of enzymes capable of digesting insoluble β -glucan, WGP is captured predominantly by gastrointestinal macrophages, where yeast glucan is digested into small active β -(1–3) glucan fragments [16]. These glucan fragments are transported by macrophages to the bone marrow, spleen and draining lymph nodes (DLNs) for interaction with immune cells [17], thus leading to the stimulation of innate and adaptive immune responses.

Our previous studies have shown that orally administered WGP β -glucan could delay tumor growth [4, 18]. In this study, we utilized WGP as vaccine adjuvant carriers to fabricate a WGP-based oral cancer vaccine loading with the model antigen ovalbumin (OVA) as reported previously [9, 19]. We hypothesized that such vaccine could induce a potent CD8^+ T cell immune response owing to the capability of targeted antigen delivery and adjuvant efficacy of WGP. Following oral administration, β -glucans first interacted with gastrointestinal macrophages; therefore, bone marrow-derived macrophages (BMDMs) were used as targeted cells to investigate the effectiveness of WGP-OVA delivery system in vitro. Thereafter, we further demonstrated the therapeutic efficacy of this oral WGP-OVA vaccine in OVA-expressing B16 melanoma and Lewis lung cancer (LLC) tumor mice models. The aim of this study was to testify whether WGP could serve as a potent adjuvant carrier for promising WGP-based therapeutic cancer vaccines.

Materials and methods

Materials

WGP, extracted from the cell walls of *Saccharomyces cerevisiae*, were kindly provided by Professor Jun Yan from the University of Louisville. Following a series of alkaline and acid extraction, cytoplasm and other cell wall polysaccharides such as mannose were removed and intact β -1,3-glucan shells were obtained. To remove any trace amounts of LPS contamination, the WGP was suspended in 200 mM NaOH for 20 min at room temperature (RT), washed thoroughly and resuspended in LPS-free water as described previously [4]. The endotoxin level was 0.06 EU/ml as tested by the gel-clot method (Associates of Cape Cod, East Falmouth, MA).

Preparation of WGP-OVA vaccine

The WGP-OVA was prepared as described previously with slight modifications [19]. Briefly, 50 mg WGP was swollen with 250 μl OVA solution (Sigma-Aldrich, China; 25 mg/ml dissolved in 0.9% NaCl) at 4 $^{\circ}\text{C}$ for 2 h for OVA diffusion into the hollow cavity of glucan particles. The wet samples were then lyophilized at -80°C to remove the water. To ensure the residual protein was added to the glucan particles, 250 μl sterile water was added to the dry samples at 4 $^{\circ}\text{C}$ for 2 h, followed by re-lyophilization. After preheating at 50 $^{\circ}\text{C}$, the dry formulations were swollen and mixed with 250 μl saturated tRNA solution (torula yeast, type VI, Sigma-Aldrich, China, 25 mg/ml dissolved in 0.9% NaCl) for 30 min at 50 $^{\circ}\text{C}$ to trap protein into the particle shells. To complete the trapping reaction, another 2500 μl tRNA solution (10 mg/ml dissolved in 0.9% NaCl) was added to the paste and incubated for 1 h at 50 $^{\circ}\text{C}$. The samples were centrifuged for 5 min, and the supernatants were collected. The pellets were washed with 0.9% NaCl three times, and the supernatants were combined with the previous supernatants for the measurement of unbound OVA using a BCA assay. The prepared WGP-OVA particles were diluted to 10 mg/ml and stored at -20°C for the following study. For the determination of the optimum encapsulation efficiency, 10 mg WGP was used to absorb 50 μl of various concentrations of OVA dissolved in 0.9% NaCl solution, followed by the lyophilization and the entrapment of OVA into WGP particles using tRNA. The WGP-BSA (bovine serum albumin) was prepared as the WGP-OVA formulation.

For phagocytosis by macrophages, FITC-labeled OVA replaced OVA for the preparation of WGP-FITC-OVA particles. For in vitro experiments, WGP and WGP-OVA particles were sonicated to produce a single-particle

suspension. WGP as controls was suspended in 200 mM NaOH for 20 min at room temperature to remove trace amounts of LPS contamination. WGP was washed completely and resuspended in sterile water as described previously [20].

Mice and tumor models

OT-I mice (transgenic OVA T-cell receptor recognized OVA-specific CD8⁺T cells) and OT-II mice (transgenic OVA T-cell receptor recognized OVA-specific CD4⁺T cells) were kindly provided by Professor Hai Qi from Tsinghua University. Female SPF C57BL/6 mice and C57BL/6 Dectin-1^{-/-} mice aged 6–8 weeks were purchased from Changzhou Cavens Company. All mice were provided free access to food and maintained under specific pathogen-free conditions. The murine tumor protocols were performed in compliance with all relevant laws and institutional guidelines and were approved by the institutional Animal Care and use Committee of Nanjing Medical University.

For the OVA-B16 tumor model, 2×10^5 cells in 100 μ l PBS were subcutaneously injected into the flanks of each mouse. After palpable tumors were formed, mice were randomly assigned to five groups and were orally administered 100 μ l OVA (containing 0.06 mg OVA), 100 μ l WGP (containing 1 mg WGP), 100 μ l WGP-BSA (containing 1 mg WGP-0.06 mg BSA) and 100 μ l WGP-OVA (containing 1 mg WGP-0.06 mg OVA) once per day, respectively. The tumor masses were measured three times per week, and the tumor dimension volumes were calculated with the formal $V = 1/2 * \text{the vertical length} * \text{the horizontal length}^2$. All mice were killed with an overdose of CO₂ in compliance with relevant laws and institutional guidelines when tumors reached 1.5 cm in diameter.

For the OVA-LLC tumor model, female C57BL/6 mice were subcutaneously implanted with 5×10^5 OVA-LLC cells. After palpable tumors were formed, mice were divided into two groups (control mice and WGP-OVA-treated mice). The WGP-OVA-treated mice were orally administered 100 μ l (10 mg/ml) WGP-OVA vaccine, while the control mice were fed normally without treatment. The tumor size was measured as described in the OVA-LLC tumor model.

Surface and intracellular staining of tumor samples and spleens

Surface and intracellular staining for lymphocytes and APCs was performed as described previously [4]. After mincing into small pieces, tumor tissues were digested with a triple enzyme mixture containing collagenase type IV, hyaluronidase and deoxyribonuclease (Sigma-Aldrich, Shanghai, China) for 30 min at 37 °C by rotation. Cells were filtered to

remove insoluble fiber, and red blood cells were lysed with red blood cell (RBC) lysis buffer (Beyotime Biotechnology, China). For surface marker staining, fluorescein-conjugated mouse-specific antibodies against CD3, CD4, CD8, Gr-1, CD11b and F4/80 (Biolegend, San Diego, CA) were used to label leukocytes. For analysis of OVA-specific CD8⁺ T cells, monocytes were incubated with the PE-anti-OVA epitope SIINFEKL (MBL International, Massachusetts, US) for 20 min at RT, followed by staining with FITC-anti-CD8 antibody (MBL International, Massachusetts, USA) for 20-min incubation at RT. The stained cells were washed with phosphate-buffered saline (PBS, Thermo Fisher Scientific Inc.) and analyzed by flow cytometry. Splenocytes were stained with specific antibodies as described above after red blood cells from single-cell suspensions were removed with RBC lysis buffer.

For intracellular staining for granzyme B, cells were surface-stained with anti-CD8 antibody, fixed, permeabilized and stained with anti-granzyme B to detect granzyme B⁺CD8⁺ T cells by flow cytometry.

To detect OVA-specific T cell responses, single-cell suspensions from tumors and spleens were restimulated with OVA (50 μ l/mg) for 4 days. The cells were then stained with anti-CD3, anti-CD4 and anti-CD8 antibodies to analyze the percentage of CD3⁺CD4⁺ T cells and CD3⁺CD8⁺ T cells by flow cytometry. For intracellular staining for IFN- γ , cells were surface-stained with anti-CD4 and anti-CD8 and then fixed and permeabilized for IFN- γ intracellular staining after restimulation with LAC (Leukocyte Activation Cocktail with BD GolgiPlug™, BD Bioscience, China) for 4 h. LAC stimulation induces the production of IFN- γ and blocks intracellular IFN- γ transport processes to enhance the detectability by flow cytometric analysis.

Bone marrow-derived macrophages (BMDMs)

Bone marrow cells isolated from the tibiae and femurs of C57BL/6 mice aged 6–8 weeks were cultured in DMEM containing 10% FBS (Thermo Fisher Scientific Inc.) supplemented with 20 ng/ml macrophage colony-stimulating factor (M-CSF). On day 3, DMEM containing 10% FBS and 20 ng/ml M-CSF was readded to generate M0 macrophages. Cultured BMDMs at day 7 were used for subsequent experiments.

Ovalbumin (OVA)-transfected B16 cells and LLC cells

OVA-expressing tumor cells were acquired according to Ca₃(PO₄)₂ transfection. Briefly, subconfluent 293 T cells cultured in DMEM supplemented with 10% FBS were added to a mixture containing CaCl₂, MSCVires vector DNA, PCLeco plasmid and HBSS for the production of pMiT-OVA retrovirus. After 2 days of cultivation,

the retrovirus in supernatants was collected and used to infect LLC cells and B16 cells obtained from American Type Culture Collection (ATCC). Tumor cells that stably expressed OVA were purified with FITC-labeled anti-OVA antibody (Abcam, UK) using FACS Melody (BD Biosciences, San Jose, CA).

In vitro cellular uptake experiments

For in vitro antigen uptake experiments, M0 BMDMs were cocultured with WGP-encapsulated FITC-labeled OVA (10 µg/ml) at 4 °C and 37 °C for 2 h. BMDMs were then harvested and stained with PE-anti-F4/80 antibody to analyze FITC signals from F4/80⁺ macrophages by flow cytometry on a FACS Canto II (BD Biosciences, San Jose, CA). To observe the uptake of WGP-OVA by BMDMs, BMDMs were cultured with WGPs encapsulated with FITC-labeled OVA for 2 h at 37 °C. PE-anti-F4/80 antibody was used to label macrophages for 15 min before the uptake profile was observed under a fluorescence microscope (Olympus IX71, JP).

To assess antigen cross-presentation of macrophages, BMDMs were pulsed with OVA (50 µg/ml), WGP-OVA (10 µg WGP-0.6 µg OVA/ml), WGP (10 µg/ml), WGP + OVA (10 µg WGP + 0.6 µg OVA/ml) and OVA (0.6 µg/ml) for 3 days, respectively. BMDMs were stained with PE-anti-SIINFEKL/H-2 Kb, and APC-anti-F4/80 antibodies were analyzed by flow cytometry.

For in vitro macrophage maturation and polarization experiments, M0 BMDMs were cultured with WGP-OVA (10 µg WGP-0.6 µg OVA/ml), WGP (10 µg/ml), WGP + OVA (10 µg WGP + 0.6 µg OVA/ml) and OVA (0.6 µg/ml) for 3 days. After treatment with various formulations, the supernatant was collected and analyzed for proinflammatory IL-6 and TNF-α using a Multi-Analyte Flow Assay kit (BioLegend, San Diego, CA) by flow cytometry, while BMDMs were stained with anti-F4/80, anti-CD80, anti-CD86, anti-MHC-I and anti-MHC-II (BioLegend, San Diego, CA) antibodies for 20 min at room temperature (RT) before analysis using flow cytometry. Total RNA from BMDMs treated with various formulations was isolated for quantitative RT-PCR amplification.

BMDM-mediated in vitro T cell proliferation and differentiation assay

CD4⁺ T cells and CD8⁺ T cells from lymph nodes and spleens of OT-II and OT-I mice were purified with magnetic-activated cell-sorting beads (Miltenyi Biotec, CN). Purified CD4⁺ T cells and CD8⁺ T cells were prelabeled with CFSE and cultured with BMDMs (T cells: BMDMs = 5:1) in the presence of various formulations in complete RPMI 1640 culture medium containing 10% FBS-supplemented amino acids and 2-mercaptoethanol. On day 5, the cells were stained with anti-CD4 and anti-CD8 antibodies for the proliferation assay. On day 7, the cells were intracellularly stained with IFN-γ as described above. Data were acquired by flow cytometry and analyzed by FlowJo software Version 7.6.1.

Immunofluorescent staining of M1 TAMs

Frozen tumor tissue sections collected from mice were fixed in ethanol containing 2% acetic acid for 30 min. After washed with running water, the frozen sections were incubated with PE-F4/80 and FITC-CD86 antibody (1:100 diluted in PBS, BioLegend, San Diego, CA) at 4 °C for 30 min in the dark. The sections were washed three times with PBS prior to the observation of CD86⁺ TAMs by fluorescence microscopy (Olympus IX71, JP).

qRT-PCR

BMDMs stimulated with various formulations and tumor samples were treated with TRIzol reagent (Invitrogen, Thermo Fisher Scientific, CN), and total RNAs were isolated and reverse-transcribed with TaqMan Reverse Transcription Reagents (Applied Biosystems, CN). The indicated cytokine mRNA levels were quantified by quantitative RT-PCR amplification using the BioRad MyiQ single color RT-PCR detection system. Briefly, complementary DNA was amplified in a 25 µl reaction mixture containing 12.5 µl SYBR Green PCR supermix (Invitrogen, Thermo Fisher Scientific, CN), 100 ng complementary DNA template and selected primer (200 nM) using the recommended cycling conditions. The primer sequences designed with Primer Express Software Version 2. (Applied Biosystems) are summarized in

Table 1 OVA encapsulation efficiency and loading ratio of OVA at various OVA concentrations

Added OVA (mg/ml)	5	10	25	50	100
OVA-loading weight ratio (OVA: WGP)	0.77:100	0.66:100	6.3:100	9.1:100	27:100
OVA encapsulation efficiency %	30.97 ± 7.64	13.20 ± 2.93	50.58 ± 1.60	36.53 ± 2.01	54.00 ± 4.11

supplemental data Table 1. Data were acquired on an ABI ViiA 7 Real-time PCR system.

Statistical analysis

Prism 8 (GraphPad software) was used to conduct statistical analysis to generate graphs of the percentage of fluorescent-positive cells or tumor growth curve. The data were analyzed using Student's *t* test to determine the significance of differences between two groups. The threshold for statistical significance was $p < 0.05$.

Results

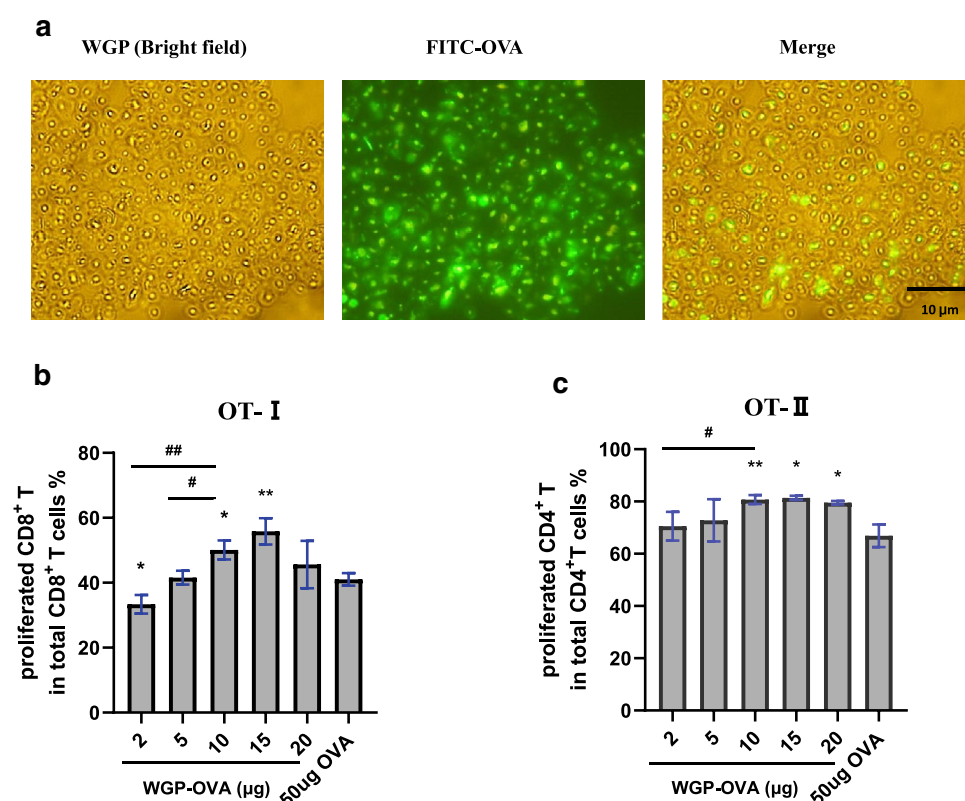
Preparation and characterization of WGP-OVA cancer vaccine

A WGP-OVA formulation was prepared as described previously [9]. To confirm the optimum encapsulation efficiency, 10 mg WGP was swollen with 50 μ l of OVA dissolved in 0.9% NaCl solution at different concentrations. It was found that OVA concentration at 25 mg/ml and 100 mg/ml showed maximal encapsulation efficiency (50%) (Table 1). Based on the “as low as reasonably achievable” (ALARA) principle, 25 mg/ml OVA with the OVA-loading ratio of 100:6.3 (1 mg WGP loading 0.06 mg

OVA) was chosen for the validation of effectiveness. The stability of prepared WGP-OVA vaccine was also determined by the detection of leaked OVA from such vaccine, and scarcely any OVA was detected within half a year when the vaccine was stored at 4 $^{\circ}$ C (Fig. S1, Supporting Information). To further confirm that OVA was encapsulated into WGP, FITC-labeled OVA was used to prepare WGP-FITC-OVA vaccine. Images from the fluorescence microscopy showed that WGP and FITC fluorescence signals were overlapped, indicating that OVA was located inside WGP (Fig. 1a).

To test whether OVA incorporated in WGP had biological functions, splenocytes and lymph node cells from transgenic OT-I mice (containing CD8⁺ T cells that are recognized by the OVA peptide in the presence of MHC-I APCs) and OT-II mice (containing CD4⁺ T cells that are recognized by the OVA peptide in the presence of MHC-II APCs) prelabeled with CFSE were incubated with OVA (50 μ g/ml), a positive control that was previously proved to induce the proliferation and differentiation of T cell effectively [4, 18], and WGP-OVA at various concentrations. The CFSE-diluted T cell population was identified as proliferating T-cells. As shown in Fig. 1b, c, WGP-OVA induced CD4⁺ T cell proliferation in a dose-dependent manner, while CD8⁺ T cell proliferation peaked when stimulated by 15 μ g WGP-OVA. Together with the capacity of inducing CD4⁺ T cell and CD8⁺ T cell proliferation

Fig. 1 Preparation and characterization of WGP-OVA vaccine. **a** WGPs encapsulated with FITC-labeled OVA was observed by fluorescence microscopy at 100 \times magnification (scale bar: 10 μ m). Single-cell suspensions from lymph nodes and spleens obtained from OT-I and OT-II mice were labeled with CFSE before incubation with 50 μ g OVA (positive control) and a different concentration of WGP-OVA. After 4 days of culture, cells were collected, and the percentages of proliferated CD8⁺ T **b** and CD4⁺ T **c** cells were assessed as shown. * $p < 0.05$, ** $p < 0.01$ compared with controls and # $p < 0.05$, ## $p < 0.01$ compared with 10 μ g WGP-OVA group.



by WGP-OVA compared with that by control OVA, 10 μg WGP-OVA (10 μg WGP loading 0.6 μg OVA) was chosen for the following in vitro experiments.

Uptake and activation of macrophages

It has been previously reported that orally administered WGP derived from the cell walls of *Saccharomyces cerevisiae* is primarily internalized by gastrointestinal macrophages via a dectin-1-dependent pathway [15]. Hence, bone marrow-derived macrophages (BMDMs) were served as target cells to confirm the cellular uptake profile of the WGP-OVA vaccine in vitro. WGP loaded with fluorescein FITC-labeled OVA particles was incubated with BMDMs at 37 °C for 2 h. After BMDMs were labeled with PE-F4/80 antibody, we found that WGP-FITC-OVA particles were engulfed by BMDMs in vitro as shown in Fig. 2a. The phagocytosis efficiency was quantified with the percentage of FITC⁺F4/80⁺ macrophages and FITC-intensity of F4/80⁺ macrophages by FACS (Fig. 2b, c). To minimize the nonspecific binding, BMDMs were co-cultured with WGP-FITC-OVA at 4 °C for 2 h, before collecting for the quantification analysis of the phagocytosis of WGP-FITC-OVA using FACS. These data confirmed that BMDMs effectively phagocytosed WGP-FITC-OVA. To further testify Dectin-1 molecule essential to recognize and uptake WGP-OVA, dectin-1-deficient BMDMs were also co-cultured with WGP-FITC-OVA under the identical condition. Not surprisingly, dectin-1-deficient BMDMs were not capable of engulfing WGP-FITC-OVA (Fig. S2a, and 2b, Supporting Information), suggesting that the phagocytosis of WGP-based vaccine by macrophages was Dectin-1-dependent.

After stimulation by microbial components such as lipopolysaccharide (LPS), immature M0 macrophages can be driven into M1-like macrophages capable of proinflammatory responses. M1 macrophages are characterized by the overexpression of CD80, CD86 and MHC molecules and the secretion of proinflammatory cytokines including IL-6, IL-12 and TNF- α [21]; therefore, we compared BMDM activation stimulated by different formulations in vitro by the detection of surface marker expression using FACS. As shown in Fig. 2d, the surface costimulatory molecules (CD80 and CD86) on macrophages were upregulated by WGP-OVA (10 μg WGP containing 0.6 μg OVA) compared with 10 μg WGP, 0.6 μg OVA alone, WGP and OVA in a cocktail manner (10 μg WGP + 0.6 μg OVA). Meanwhile, WGP-OVA also remarkably enhanced the expression of MHC-I and MHC-II molecules that are associated with antigen presentation. In addition, both the mRNA and protein levels of typical cytokines TNF- α and IL-6 expressed on M1 macrophages were elevated by the WGP-OVA vaccine (Fig. 2e, f). Notably, WGP alone was able to induce not only the upregulation of costimulatory molecules, including CD86, MHC-I

and MHC-II, but also the secretion of TNF- α , suggesting that WGP alone had an adjuvant potential, and loaded model antigen OVA further amplified immune responses to promote the strongest M1 macrophage polarization.

The OVA₂₅₇₋₂₆₄ peptide (SIINFEKL) complexed with major histocompatibility complex (MHC-I) molecules is required for the initiation of cross-priming CD8⁺ T cell responses [22, 23]. The FACS results revealed that WGP-OVA induced the highest percentage of F4/80⁺SIINFEKL⁺ macrophages after treatment for 48 h (Fig. 2g). These results demonstrated that WGP encapsulated with OVA enhanced the highest level of SIINFEKL peptides on the surface of macrophages, and achieving levels much higher than those observed after other formulation treatments, indicating that WGP could function as a targeting carrier to promote antigen delivery.

Proliferation and differentiation of T cells stimulated by WGP-OVA in vitro

The activation of T cells induced by cancer vaccines is the main cause of the destruction of cancer cells [24]. We hence evaluated the potential of the WGP-OVA vaccine to prime both CD4⁺ T cells and CD8⁺ T cells in vitro. CD4⁺ T cells purified from the spleens and lymph nodes of OT-II mice and CD8⁺ T cells purified from the spleens and lymph nodes of OT-I mice were cultured with BMDMs (T cells: BMDM = 5:1), and then, different formulations were added for the analysis of the proliferation and differentiation of T cells. As shown in Fig. 3a, c, only 0.6 μg OVA encapsulated in 10 μg WGP was sufficient to induce the proliferation of CD4⁺ T cells and CD8⁺ T cells similar to 50 μg OVA, as assessed by CFSE dilution assay. However, equal doses of WGP or OVA, as well as WGP and OVA in a cocktail manner, were unable to induce the proliferation of T cells. After 7 days of culture, the percentages of IFN- γ ⁺ T cells were assessed using FACS to determine the differentiation of T cells. As shown in Fig. 3b, d, both 50 μg OVA and 10 μg WGP-OVA vaccine induced only a slight increase in IFN- γ -producing CD8⁺ T cells, while a dramatic increase in IFN- γ ⁺CD4⁺ T cells (Th1 cells) was induced by 50 μg OVA and 10 μg WGP-OVA. The ability of 50 μg OVA and 10 μg WGP-0.6 μg OVA to induce T cell expansion and differentiation showed no significant variation, indicating that with the aid of 10 μg WGP, only 0.6 μg OVA had a similar effect induced by 50 μg OVA, which verified the effect of WGP as a targeted delivery system.

Orally administrated WGP-OVA vaccine inhibits the growth of B16-OVA in vivo

Subsequently, we investigated the in vivo antitumor effect of WGP-OVA in C57BL/6 mice bearing OVA-expressing

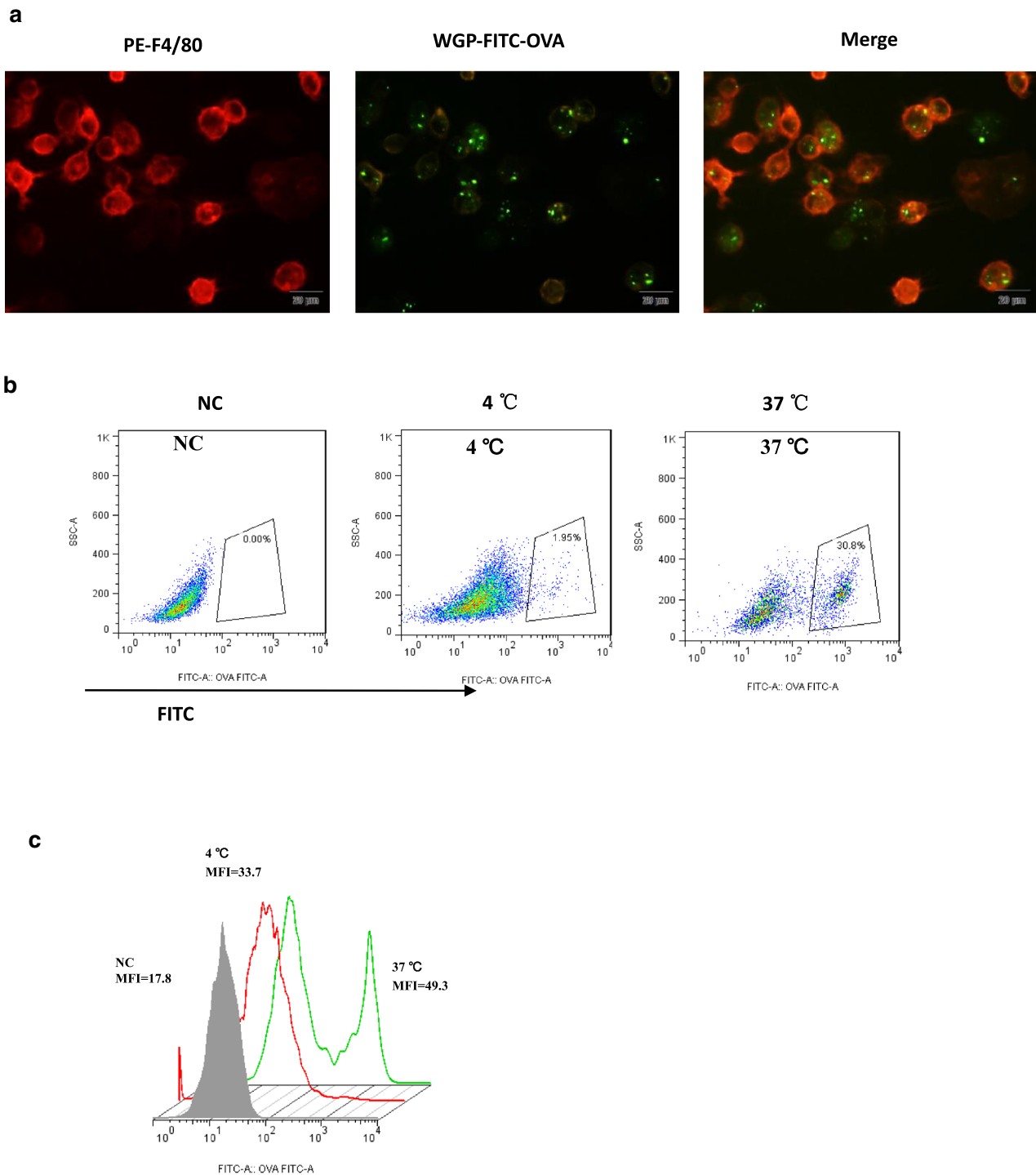


Fig. 2 Bone marrow-derived macrophage (BMDM) activation stimulated by the WGP-OVA vaccine in vitro. Representative fluorescence microscopy images of WGP-FITC-OVA uptake by BMDMs were obtained at 40× magnification. (BMDMs were stained with PE-F4/80 mAbs, and red circles represent macrophages, scale bar: 20 μm). **b** WGP (10 μg) encapsulated with FITC-labeled OVA was cultured with BMDMs for 2 h at 4 °C and 37 °C, respectively. FITC⁺F4/80⁺ BMDMs % was detected by FACS to quantify the efficiency of uptake. **c** The uptake effect was confirmed by FITC fluorescence

intensity using FACS. **d** BMDMs were cocultured with different formulations for 48 h, and surface marker expression was assessed by FACS analysis. Gene expression and protein production of TNF-α **e**) and IL-6 **f**) were analyzed by qRT-PCR and a Multi-Analyte Flow Assay Kit using FACS from BMDMs stimulated by four formulations, respectively. **g** The OVA antigen cross-presentation efficiency was demonstrated as SIINFEKL⁺F4/80⁺ BMDMs % by FACS. * $p < 0.05$, ** $p < 0.01$ compared with controls and # $p < 0.05$, ## denotes $p < 0.01$ compared with WGP-OVA group

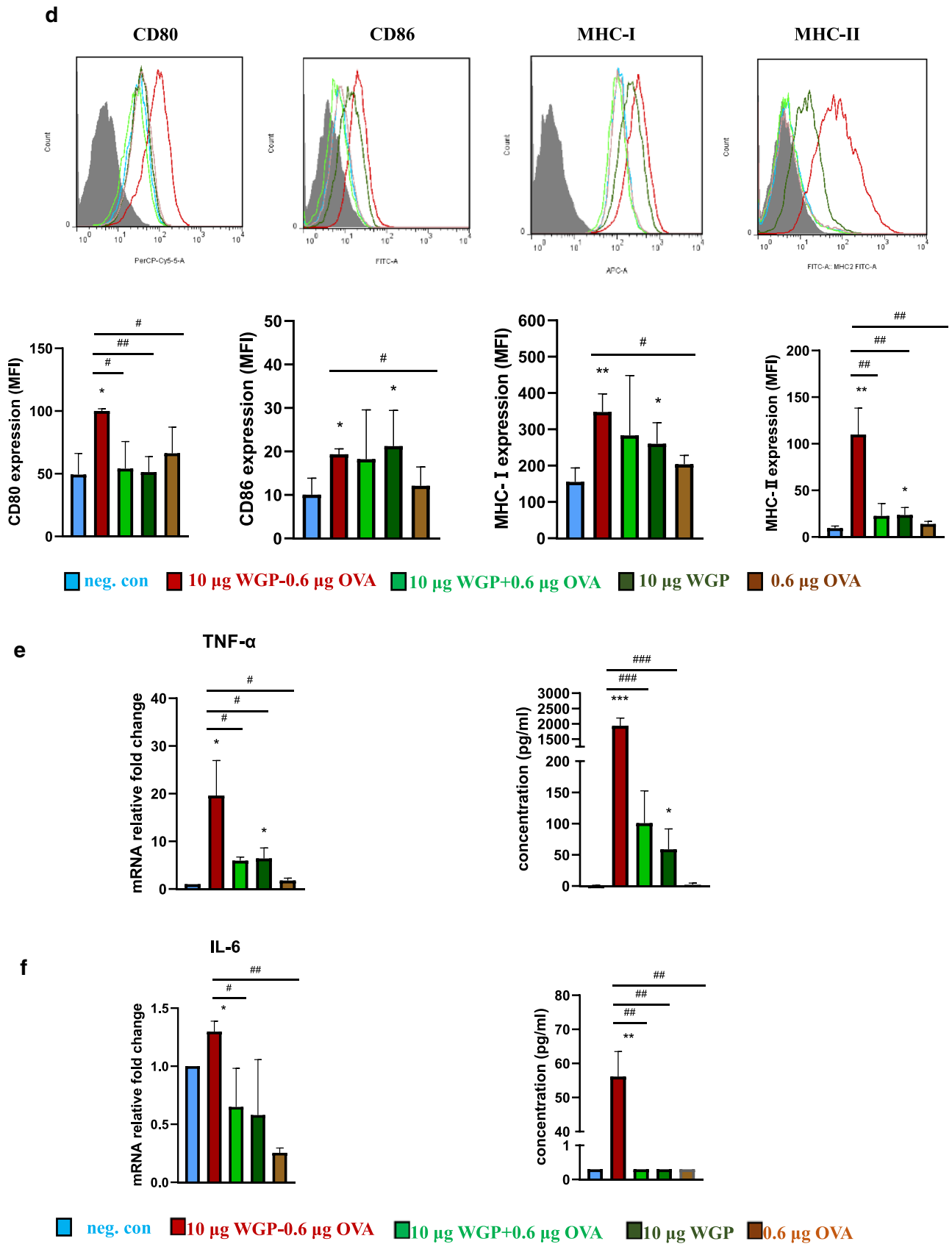


Fig. 2 (continued)

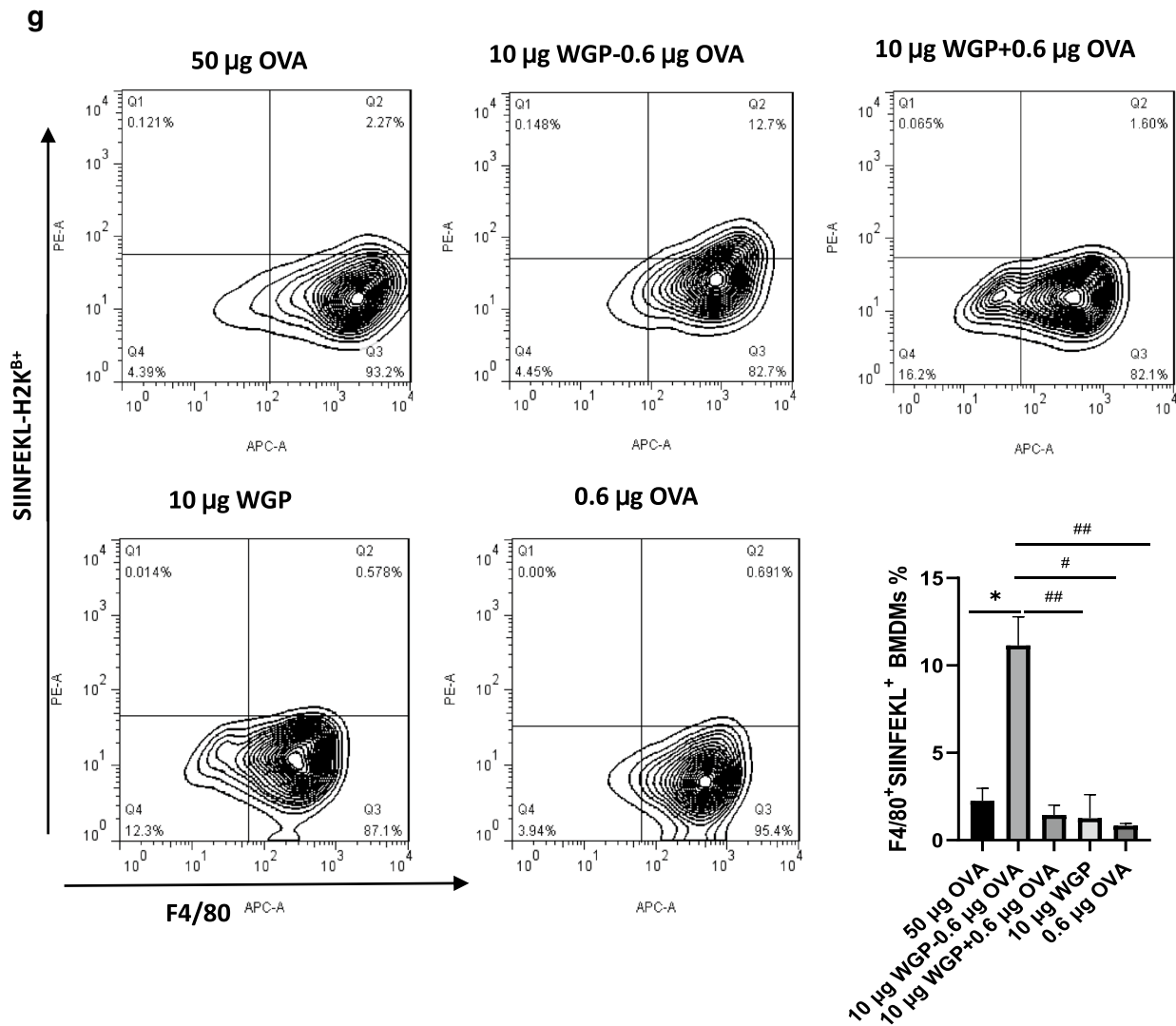


Fig. 2 (continued)

B16-OVA melanoma. The treated mice were orally administered with 100 µl OVA (containing 0.06 mg OVA), 100 µl WGP (containing 1 mg WGP), 100 µl WGP-BSA (containing 1 mg WGP-0.06 mg BSA) and 100 µl WGP-OVA (containing 1 mg WGP-0.06 mg OVA) daily until the end of the experiment, respectively (Fig. 4a). Mice receiving oral treatment with WGP loading with irrelevant antigen BSA (WGP-BSA) were used to analyze the nonspecificity of the anti-tumor response. Compared to the untreated control and OVA group, WGP, WGP-BSA, WGP-OVA vaccine all significantly delayed tumor progression. Oral administered naked OVA failed to suppress the tumor growth as expected. Mice treated with either WGP or WGP-BSA had slower tumor growth and even tumor shrinkage when compared to untreated mice; however, there was no significant difference in tumor size after the last treatment between these two

groups (Fig. 4b, c). As shown in Fig. 4d, the untreated and OVA-treated mice all died within 22 days. Benefiting from effective tumor suppression, WGP, WGP-BSA, WGP-OVA treatment resulted in longer overall survivals, and even 80% of the mice receiving WGP-OVA still alive on day 22 after the tumor inoculation.

We then studied the mechanisms underlying the therapeutic effect of the WGP-OVA formulation. Generally, T cells rapidly proliferate upon the second exposure to the same antigen, thus leading to T cell-mediated immune responses for the elimination of tumor cells [25]. Therefore, we expected that T cells from WGP-OVA-treated mice would expand, and the proliferation capability of T cells in the tumor samples and spleens from the 3 groups of mice was then analyzed by OVA stimulation (50 µg/ml) for 4 days in vitro. On the basis of FACS results, the percentages of

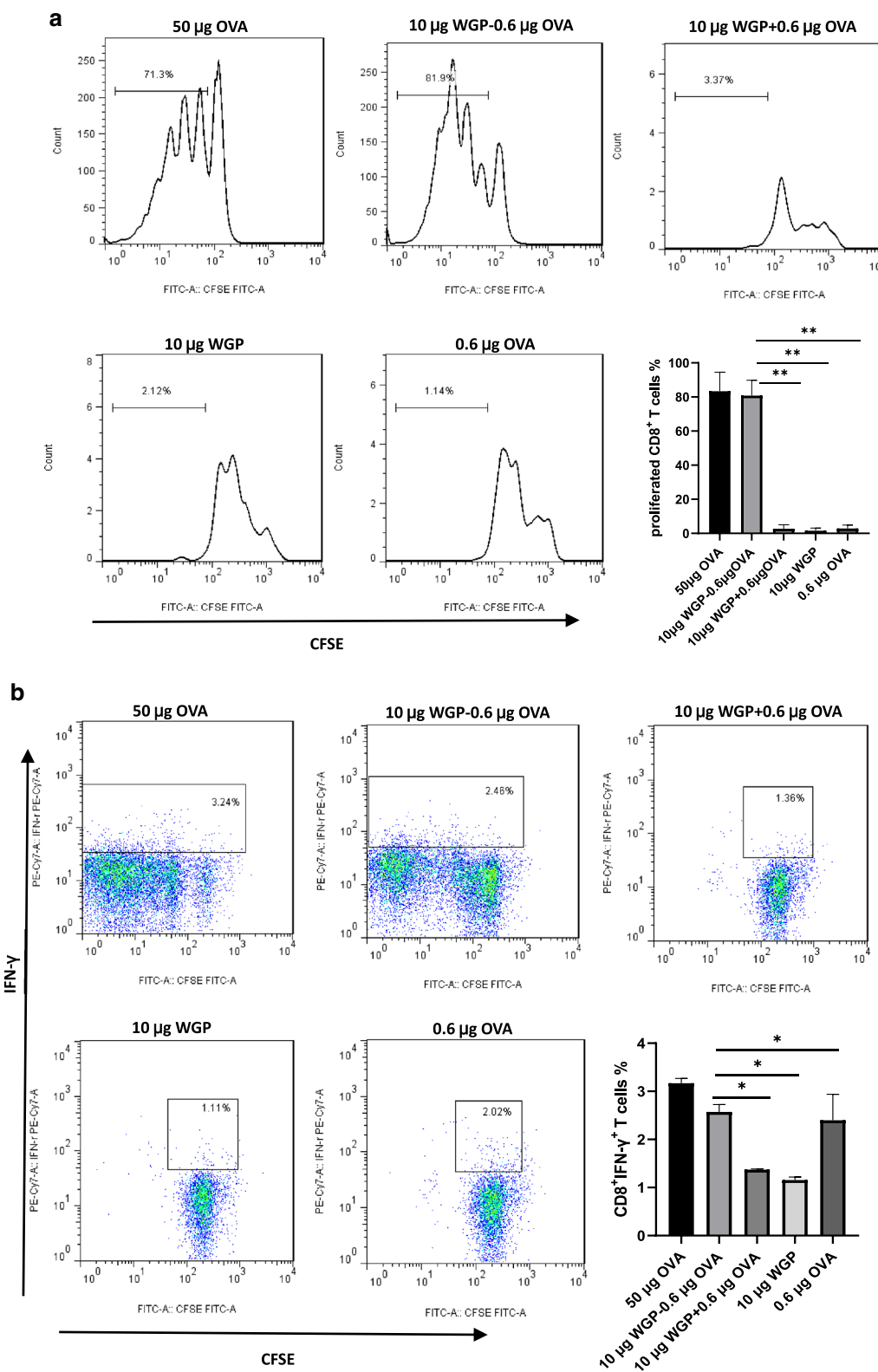


Fig. 3 The proliferation and differentiation of CD8⁺ T and CD4⁺ T cells from OT-I and OT-II mice in the presence of BMDMs stimulated by various formulations in vitro. **a** CFSE-labeled CD8⁺ T cells mixed with BMDMs were cocultured with different formulations for 4 days. **b** After culturing for 7 days, the cells were restimulated with LAC for 4 h, and proliferated IFN-γ⁺CD8⁺ T cells were analyzed by

FACS based on intracellular staining. **c** CFSE-labeled CD4⁺ T cells mixed with BMDMs were cocultured with different formulations for 4 days. **d** After culturing for 7 days, the cells were restimulated with LAC for 4 h, and IFN-γ⁺CD4⁺ T cells were analyzed by FACS based on intracellular staining. **p* < 0.05, ***p* < 0.01

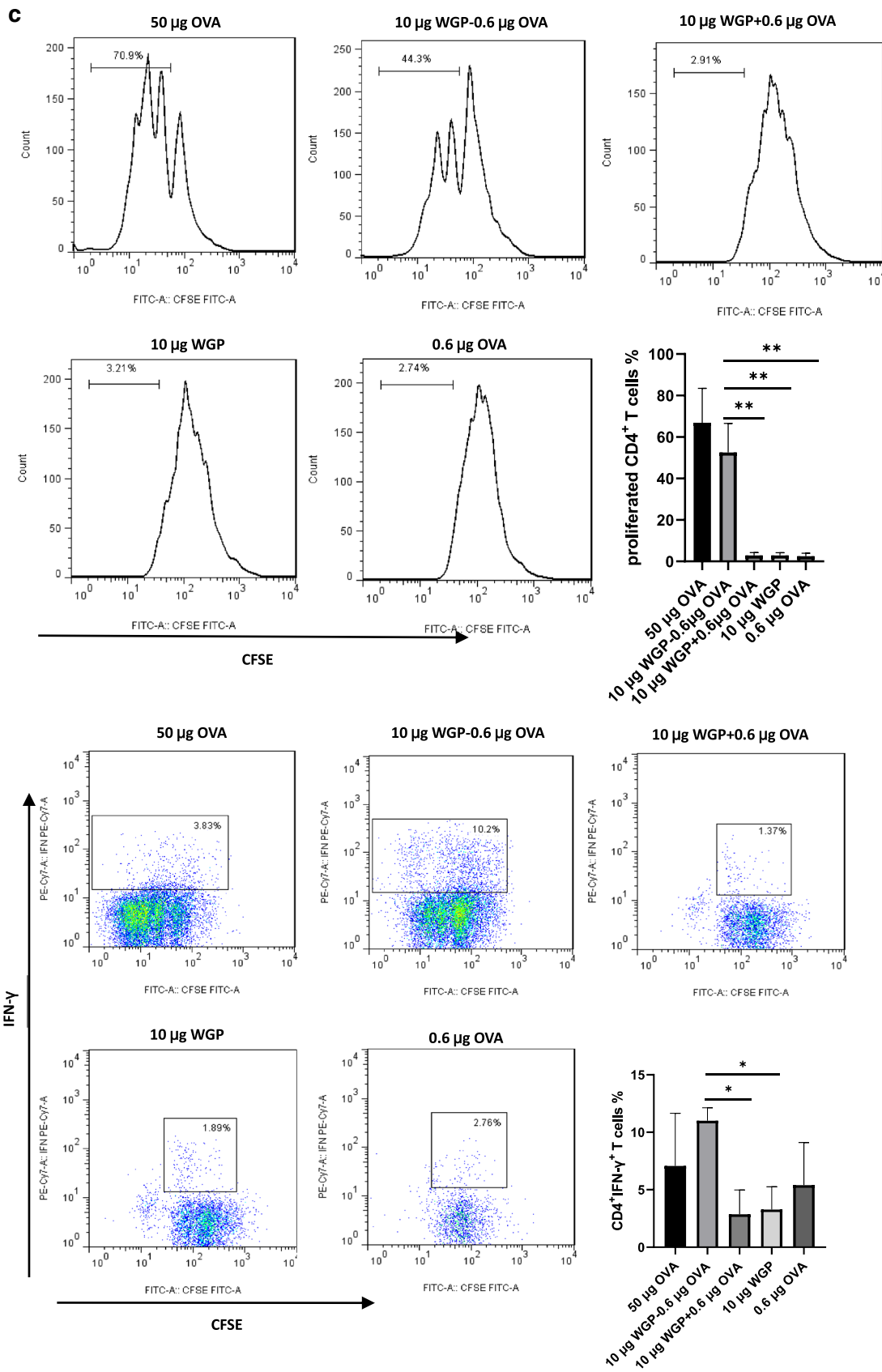


Fig. 3 (continued)

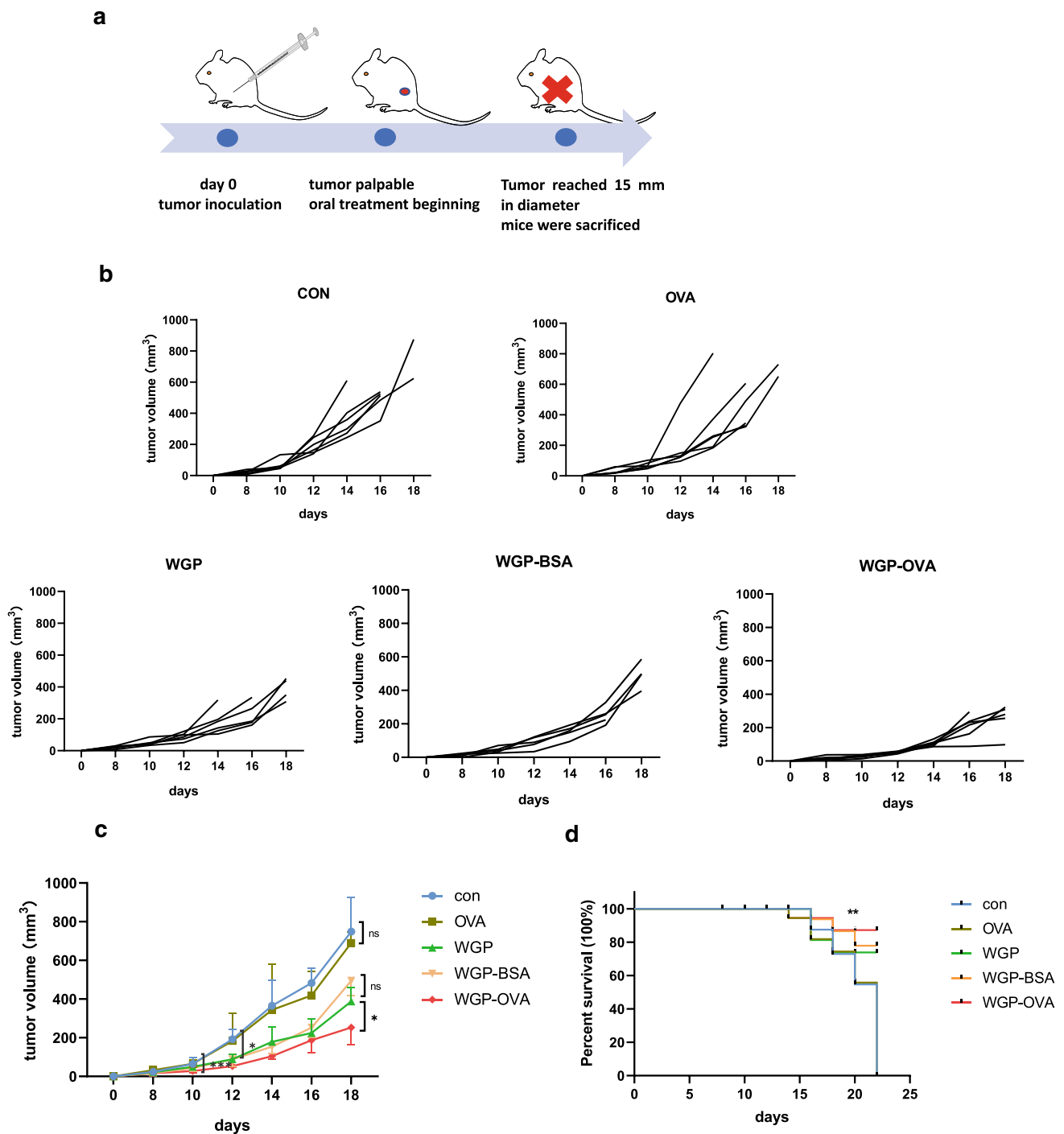


Fig. 4 WGP-OVA oral vaccine suppressed B16-OVA tumor growth in C57BL/6 mice. B16-OVA cells (2×10^5) were suspended in 0.1 ml PBS and injected subcutaneously into C57BL/6 female mice. After tumors were palpable, four groups of treated mice received oral medication of 100 μ l OVA (containing 0.06 mg OVA), 100 μ l WGP (containing 1 mg WGP), 100 μ l WGP-BSA (containing 1 mg WGP-0.06 mg BSA) and 100 μ l WGP-OVA (containing 1 mg WGP-0.06 mg OVA) daily until the end of the experiment, respec-

tively; control mice were fed as usual without additional treatment. **a** Scheme of the experimental design to evaluate the therapeutic effect of the oral medication. Individual **b** and average **c** tumor volumes were calculated by the vertical length and the horizontal length measured every two days, and tumor growth curves were plotted as indicated. **d** Survival curves for different treatment groups (max. diameter ≥ 15 mm was considered to the death, $n = 8$ for each group). * $p < 0.05$, ** $p < 0.01$

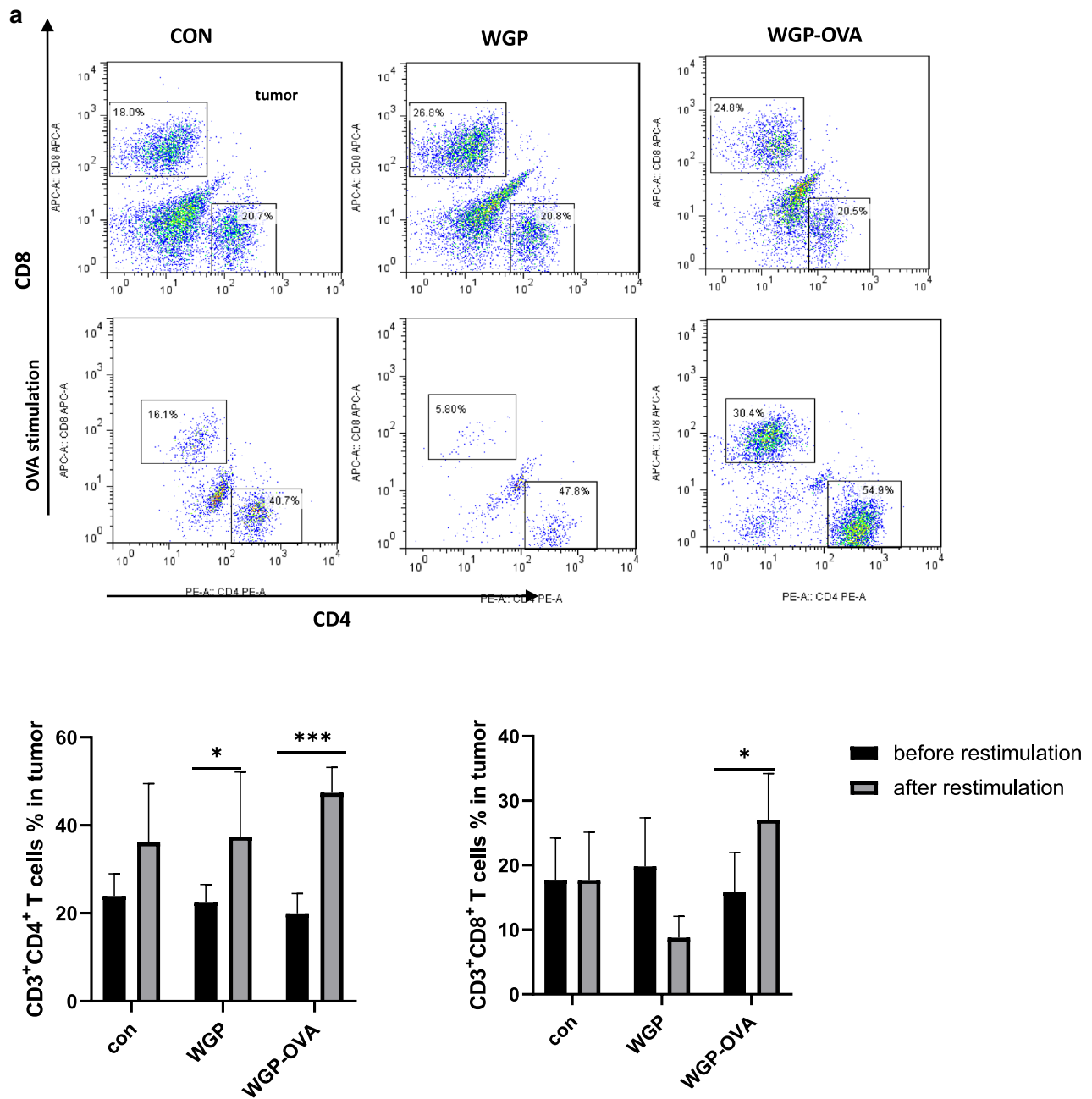


Fig. 5 WGP-OVA triggered robust antitumor immunity. **a** Single-cell suspensions from tumor tissues were restimulated with OVA (50 µg/ml) for 4 days, and CD3⁺CD4⁺ T cells and CD3⁺CD8⁺ T cells were identified with specific mAbs and analyzed by FACS. **b** Single-cell suspensions from tumor tissues were stained with diverse fluorescein-labeled mAbs to identify tetramer⁺CD8⁺ T cells. **c** Single-cell suspensions from tumor tissues of three groups of mice were intracellularly stained with anti-granzyme B mAbs and analyzed by FACS.

d Populations of tumor-infiltrating CD11b⁺F4/80⁺ macrophages from the three groups of mice were stained with specific mAbs and analyzed by FACS analysis. **e** CD86 expressions (MFI) on tumor-infiltrating CD11b⁺F4/80⁺ macrophages were assessed by FACS analysis. **f** Immunofluorescence images of CD86⁺F4/80⁺ macrophages in tumor tissues from three groups of mice at 4×magnification (scale bar: 200 µm). **p*<0.05, ***p*<0.01, ****p*<0.001

both CD3⁺CD4⁺ T and CD3⁺CD8⁺ T cells in tumors from WGP-OVA-treated mice dramatically increased compared to those from the other two groups of mice (Fig. 5a), while

this significant difference in the proliferation of splenic T cells from three groups of mice after OVA restimulation was not found (Fig. S3a, Supporting Information).

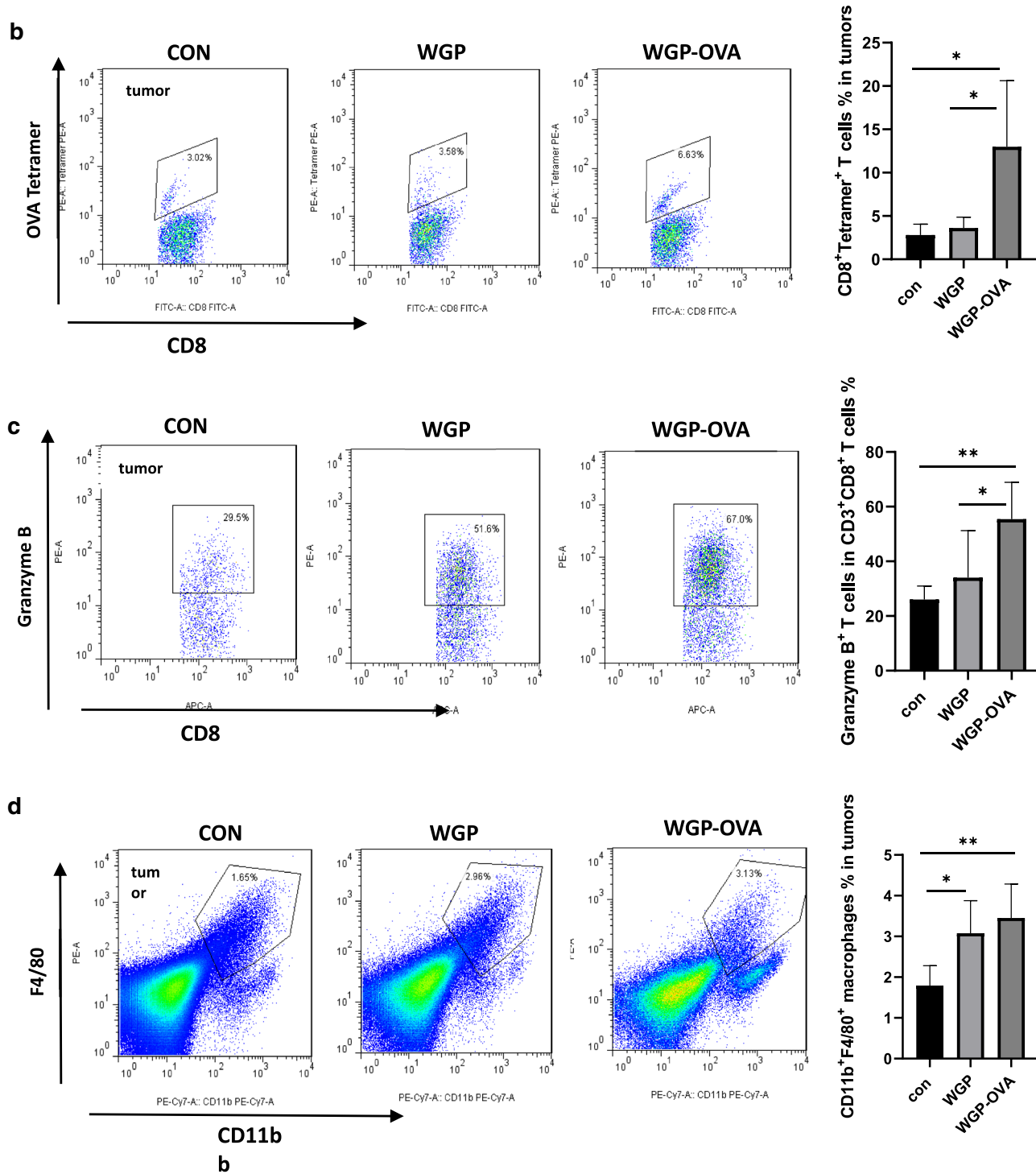
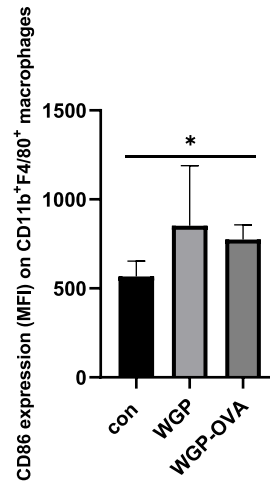
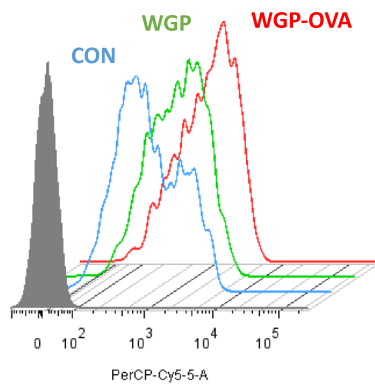


Fig. 5 (continued)

Then, we investigated the tumor-infiltrating T cell level after oral immunization and found a remarkable increase

in OVA-specific CD8⁺ T cell levels in the tumors of mice

e



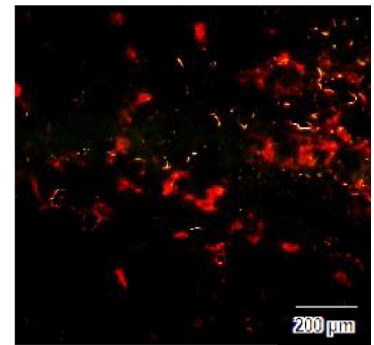
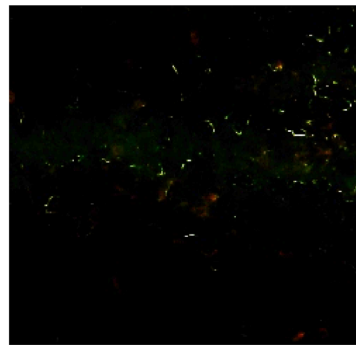
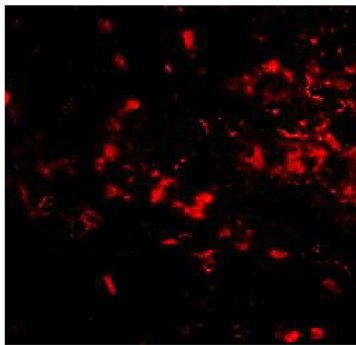
f

PE-F4/80

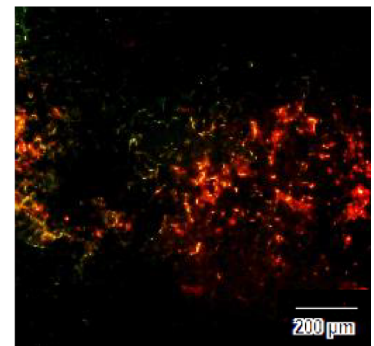
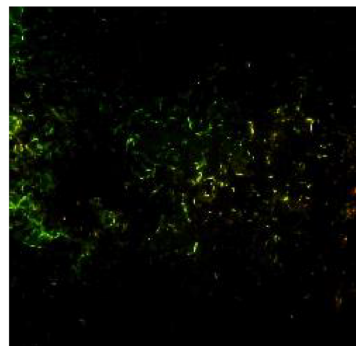
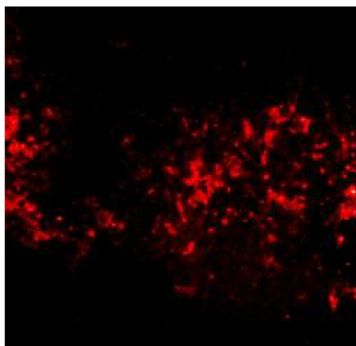
FITC-CD86

Merge

CON



WGP



WGP-OVA

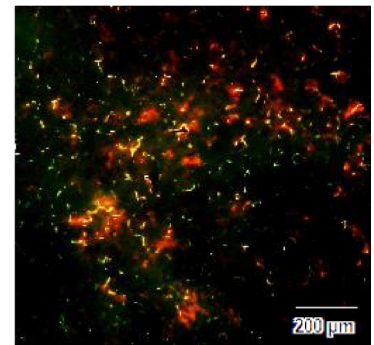
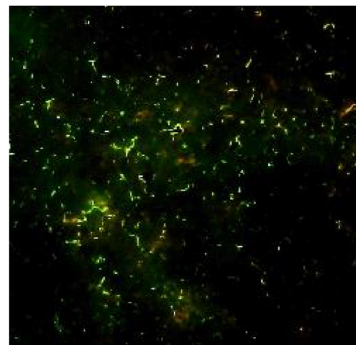
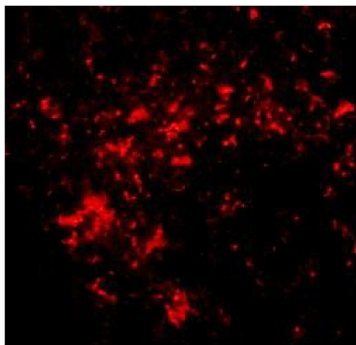


Fig. 5 (continued)

orally administered the WGP-OVA vaccine using a tetramer conjugate for the OVA epitope SIINFEKL (Fig. 5b), which was mainly ascribed to antigen cross-presentation by macrophages and DCs [26]. Granzyme B found in the cytotoxic granules of T lymphocytes plays an essential role in inducing apoptosis of tumor cells. FACS analysis revealed that intratumoral CD8⁺ T cells expressed the highest level of granzyme B from mice orally immunized with WGP-OVA (Fig. 5c). The immune checkpoint protein PD-1, which is expressed widely on activated T cells and B cells, is responsible for the failure of cancer immunotherapy [27]. However, WGP-OVA was unable to decrease the population of both PD-1⁺CD4⁺ T cells and PD-1⁺CD8⁺ T cells (Fig. S3b, Supporting Information).

We further examined tumor-infiltrating CD11b⁺ myeloid-derived immune cells. The numbers of CD11b⁺F4/80⁺ macrophages (Fig. 5d) in the tumors of mice treated with WGP-OVA were significantly increased compared to those of the control mice. Both WGP treatment and WGP-OVA treatment induced a comparable increase in intratumoral and intrasplenic CD11b⁺CD11c⁺ DCs (Fig. S3c, Supporting Information) and CD11b⁺Gr-1^{high} granulocytes (Fig. S3d, Supporting Information), which is consistent with the results of our previous study [4, 18]. M1 TAMs highly expressing CD80 and CD86 have been considered as promising therapeutic targets owing to their antitumor effects. Flow cytometry results demonstrated that F4/80⁺CD11b⁺ TAMs had higher expression of CD86 after treatment with WGP-OVA (Fig. 5e). Moreover, markedly increased CD86⁺F4/80⁺ TAMs were also observed after treatment with WGP-OVA using immunofluorescent staining (Fig. 5f), indicating that WGP-OVA could induce repolarization of TAMs toward antitumor M1-type. Taken together, these data indicated that WGP-OVA could increase the M1 TAMs infiltration and further promote antigen presentation to elicit robust antitumor immunity to prevent tumor growth.

WGP-OVA oral vaccine used in Lewis lung cancer (LLC) model

We then evaluated the effectiveness of the WGP-OVA vaccine in OVA-expressing Lewis lung cancer (OVA-LLC) tumor model. As shown in LLC-OVA tumor model, mice orally administered WGP-OVA daily had slower tumor growth than the mice without treatment (Fig. 6a, b). The survival rate of mice treated with WGP-OVA was remarkably improved compared to untreated mice (Fig. 6c). To study the mechanisms of the great antitumor effects, tumors and spleens from the two groups of mice were prepared as single-cell suspensions for FACS analysis. Consistent with the data in the B16-OVA tumor model, WGP-OVA could induce the proliferation of tumor-infiltrating OVA-specific CD8⁺ T cells (OVA-Tetramer⁺CD8⁺ T cells) (Fig. 6d); however, it

had no substantial effect on the total amount of intratumoral and intrasplenic CD4⁺ T cells and CD8⁺ T cells (Fig. S4a, Supporting Information). The percentage of tumor-infiltrating CD8⁺ T cells producing granzyme B was dramatically increased after OVA-LLC-bearing mice were treated with the oral WGP-OVA vaccine on a daily basis (Fig. 6e). The generation of granzyme B was confirmed by an increase in the mRNA level of granzyme B in the tumors from WGP-OVA-treated mice (Fig. S4b, Supporting Information). As determined by intracellular staining with anti-IFN- γ mAbs, WGP-OVA vaccine drastically increased the frequency of IFN- γ -producing CD4⁺ T cells and IFN- γ -producing CD8⁺ T cells in tumors (Fig. 6f), while there was no difference in IFN- γ -producing T cells in the spleens from the two groups of mice (Fig. S4c, Supporting Information).

At last, we examined whether the infiltration profile of CD11b⁺F4/80⁺ macrophages and CD11b⁺Gr-1^{high} granulocytes in the tumor milieu and spleens would be altered upon WGP-OVA oral administration. The frequencies of CD11b⁺F4/80⁺ macrophages (Fig. 6g and Fig. S4d, Supporting Information) and CD11b⁺Gr-1^{high} granulocytes (Fig. S4e, Supporting Information) in the tumors and spleens were both significantly increased in the WGP-OVA-treated mice. Combined with the results in OVA-B16 melanoma model, WGP-OVA was capable of enhancing the infiltration of myeloid-derived immune cells, increasing antigen-specific CD8⁺ CTLs and promoting the generation of granzyme B from CTLs to eliminate tumor cells.

Discussion

Cancer vaccination, as one of the current immunotherapies, is able to induce the desired cellular immune response against cancers. An effective tumor vaccine should satisfy the following key requirements. First, exogenous tumor antigens loaded in vaccines should be delivered to the cytosol of APCs such as DCs, macrophages and neutrophils, where antigens are processed into antigen peptides. Subsequently, these antigen peptides are presented to the surfaces of APCs by the cross-presenting pathway for the formation of complexes with major histocompatibility complex class I (MHC-I) [22]. Finally, cytotoxic T lymphocytes (CTLs) infiltrate into the tumor and these complexes within a proinflammatory environment induced by the adjuvant bound to vaccines for tumor cell killing [28]. However, a number of cancer trials have shown negative outcomes, which were partly due to the lack of an effective delivery carrier to targeted cells or organs and the adjuvant incapable of altering the immunosuppressive tumor microenvironment toward a proinflammatory environment. Therefore, the wide use of various delivery approaches, including nanoparticles [29], self-assembled materials [30, 31] and biomaterials [23], in

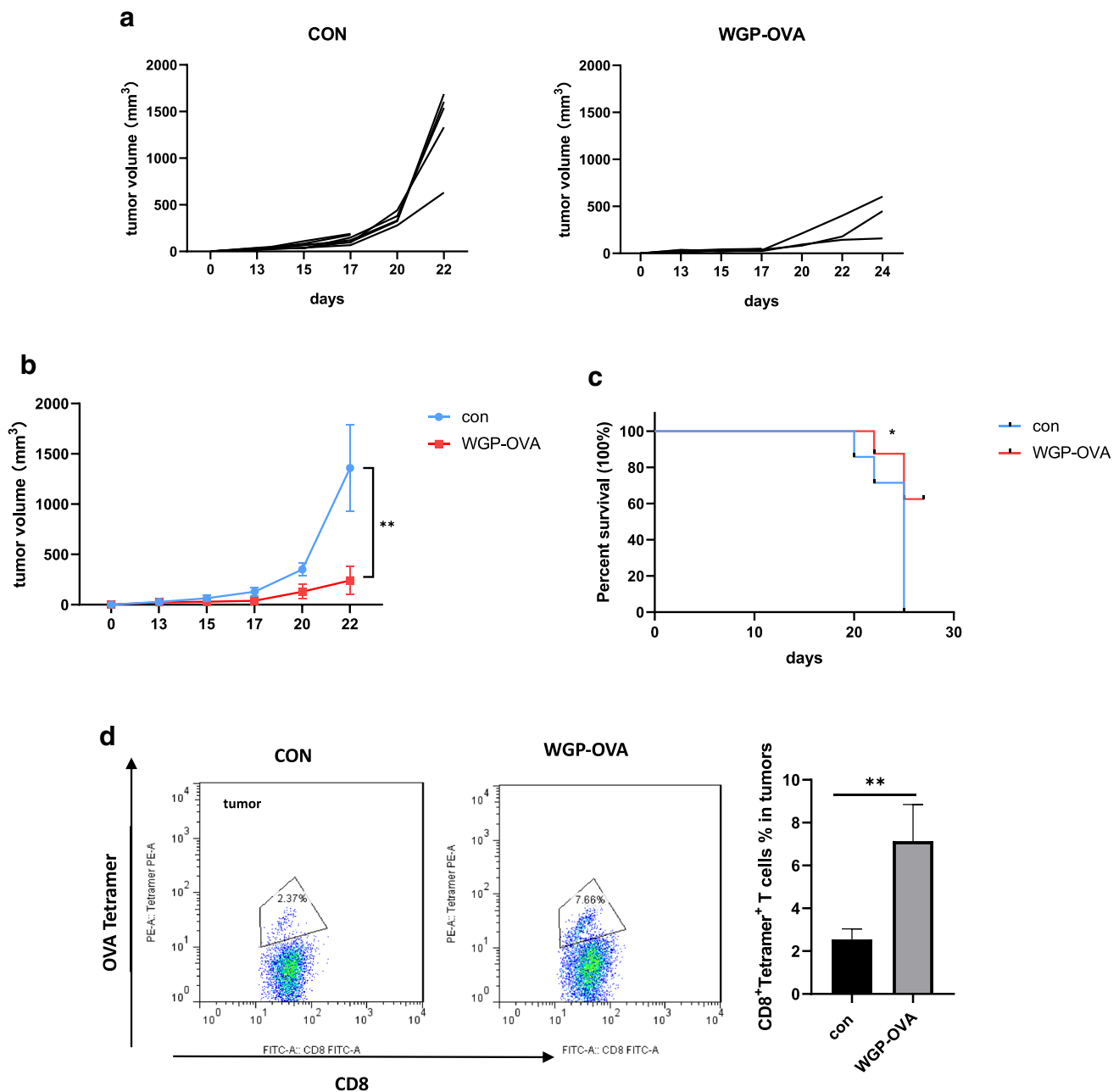


Fig. 6 The WGP-OVA oral vaccine reduced the LLC-OVA tumor burden in C57BL/6 mice. LLC-OVA cells (5×10^5) were suspended in 0.1 ml PBS and injected subcutaneously into C57BL/6 female mice. After tumors were palpable, mice were divided into a control group and a WGP-OVA orally treated group. Individual **a**) and average **b**) tumor volumes were measured with 2-day intervals and tumor growth curves were plotted as indicated. **c** Survival curves for different treatment groups (max. diameter ≥ 15 mm was considered to the death, $n = 7$ for each group). **d** FACS profile of intratumoral OVA-specific CD8⁺ T cells from the two groups of mice. **e** Single-cell sus-

pensions were prepared from tumors of the control mice and treated mice for intracellular staining. CD8⁺ granzyme B⁺ T cells were analyzed by FACS after permeabilization. **f** Tumor-infiltrating CD4⁺ T cells and CD8⁺ T cells were restimulated with PMA and ionomycin for 4 h, and IFN- γ ⁺CD4⁺ T cells and IFN- γ ⁺CD8⁺ T cells were analyzed followed by intracellular staining with anti-IFN- γ mAbs. **g** Tumor-infiltrating CD11b⁺F4/80⁺ macrophages from two groups of mice were stained with specific mAbs and analyzed by FACS. * $p < 0.05$, ** $p < 0.01$

combination with various cancer adjuvants, such as immunopotentiators, carbohydrate-based adjuvants, cytokines and

bacterial products [1], has greatly promoted the development of cancer vaccines.

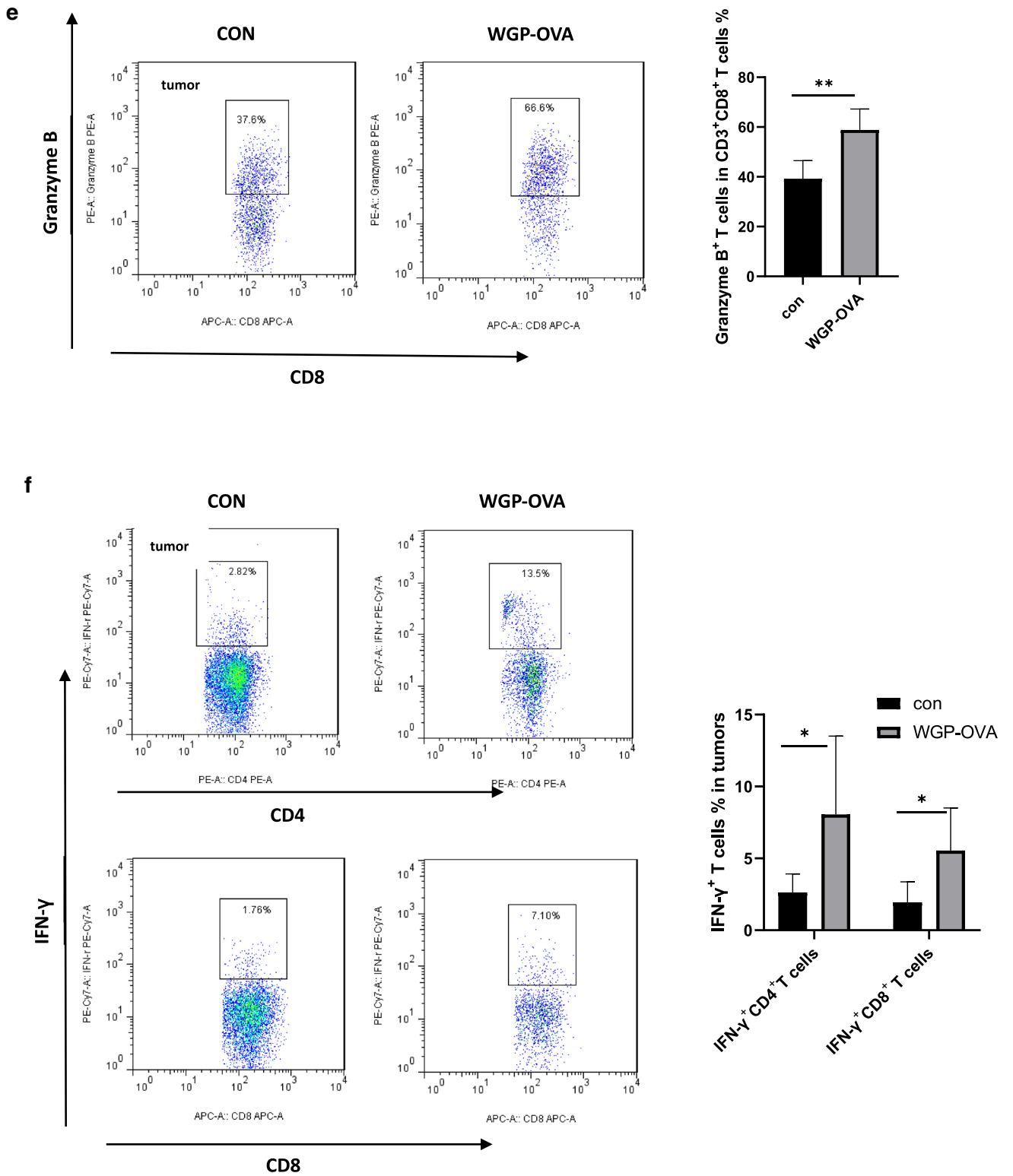


Fig. 6 (continued)

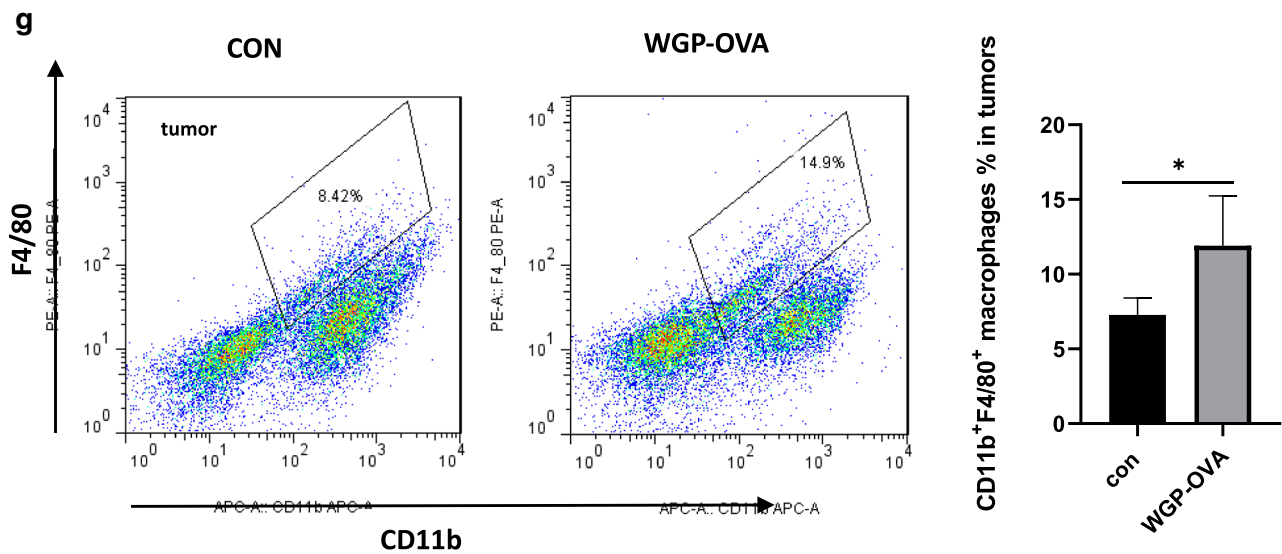


Fig. 6 (continued)

In this study, we took advantage of the specific structure of glucan particles to absorb the model antigen OVA into the hollow cavity of WGP, thus developing a WGP-based cancer vaccine. Compared with novel delivery materials, WGP is approved by the FDA as GRAS (generally recognized as safe) owing to its absence of toxicity and negative side effects to humans and thus could serve as a promising antigen-delivering carrier of cancer vaccines for clinical translation. The maximum OVA encapsulation efficiency in our experiment reached 50%, much lower than the expected encapsulation efficiency measured previously [9], probably because the extraction method of glucan particles from *S. cerevisiae* was different from that in a previous report. WGP possesses a strong adjuvant nature because of the polymer composition of β -1,3-D-glucan, which is easily detected by dectin-1 expressed on the surface of APCs, thereby inducing immunologic responses in mammals. Herein, we focused on the mechanism of the antitumor function triggered by an oral WGP-OVA targeting macrophages. After phagocytosis of WGP-OVA particles by BMDMs, the WGP carrier was degraded into active β -1–3-glucan fragments in the endosomes of macrophages, and these active moieties were subsequently released from macrophages [16] to exert immune adjuvant functions, such as driving immature M0 macrophages into M1-like macrophages capable of proinflammatory responses [32], which was confirmed by the secretion of proinflammatory cytokines TNF- α and IL-6, as indicated in Fig. 2e, f. The processing of OVA trapped in WGP has two different pathways: OVA was degraded in the proteasomes of macrophages and later displayed on the surface to form MHC-I-OVA peptides for the initiation of CD8⁺ CTL immune responses (cross-presentation pathway);

OVA was degraded in endosomes, and antigenic peptides were presented by MHC-II molecules expressed on the surface of macrophages to induce CD4⁺ Th cell-mediated immunity (endosome pathway) [33]. Here, we found that WGP-OVA induced the highest expression of MHC-I and MHC-II in BMDMs in vitro compared to WGP mixed with OVA and WGP alone, thereby promoting efficient antigen presentation for cellular immunity. These results were also confirmed by the study on the capacity for proliferation and differentiation of T lymphocytes stimulated by WGP-OVA in the presence of BMDMs in vitro (Fig. 3). While CD8⁺ CTLs, as classic cytotoxic effector cells, play a direct role in eliminating tumor cells, CD4⁺ T cells are also capable of inducing immune-mediated tumor control through various mechanisms [34], such as enhancing antigen presentation [35, 36] and costimulation [37, 38], inducing T cell homing [39] and exerting direct antitumor functions by the expression of granzymes, perforin and FasL [40]. We found that when cocultured with BMDMs as APCs, WGP-OVA not only promoted the proliferation of CD4⁺ T cells and CD8⁺ T cells but also induced naïve CD4⁺ T cells from OT-II mice to differentiate into Th1 cells, which may help naïve CD8⁺ T cells differentiate into effector CTLs. It is worth noting that with the aid of 10 μ g WGP, only 0.6 μ g OVA had a similar effect induced by 50 μ g OVA, which verified the dual effect of WGP as a targeted delivery system and adjuvant system.

It has been reported that oral WGP could control tumor development, as activated DCs caused by WGP treatment are capable of capturing apoptotic tumor cells and subsequently lead to antigen-specific CD4⁺ T and CD8⁺ T cell responses [18, 41]. Based on the previous results and the evidence from our in vitro experiments, we further

evaluated the therapeutic effect of the oral WGP-OVA in an OVA-transfected tumor models. As expected, tumor-bearing mice given oral WGP-OVA treatment exhibited the smallest tumor burden compared to those treated with WGP alone or without treatment. A similar phenotype was observed in the OVA-expressing B16 tumor model. The main reason for tumor regression caused by WGP-OVA treatment is the significant increase in the frequency of tumor-infiltrating OVA-specific CD8⁺ T cells, which was mainly ascribed to antigen cross-presentation by macrophages and DCs [26]. These effector CD8⁺ CTLs release granzyme B, a serine protease contained in cytoplasmic granules of cytotoxic T cells, which is closely related to the CTL-killing mechanism of tumor cell apoptosis because of its capacity to interfere with chromatin condensation and to disintegrate the DNA of targeted cells [42]. The killing mechanism was also confirmed by the increased number of granzyme B⁺CD8⁺ T cells in tumors.

After oral administration of the WGP-OVA vaccine, gastrointestinal macrophages, as preferential target cells, could capture and internalize WGP-OVA particles. Here, we also found that both WGP and WGP-OVA *in vivo* treatment could stimulate the expansion of CD11b⁺F4/80⁺ macrophages, CD11b⁺CD11c⁺ DCs and CD11b⁺Gr-1^{high} granulocytes in the tumor issues, which is consistent with the notion that digested WGP fragments from gastrointestinal macrophages functioning as adjuvants could induce the migration of immune cell into tumor sites [43] to enhance antigen presentation and prime T cell immune responses. It should be pointed out that WGP-OVA could effectively induce TAM-repolarization toward M1 TAMs (CD86⁺F480⁺ macrophages) in OVA-B16 mouse model, synergistically triggering antitumor T cell immunity.

Expression of immune checkpoint proteins such as PD-1 on T cells is the main cause of T cell exhaustion, which leads to the failure of the immune system to eliminate antigenic malignant cells [27]. Therefore, the use of antibodies against PD-1 or its ligand can rescue the function of exhausted T cells to fight against tumor cells [44, 45]. Recently, increasing numbers of studies focused on cancer vaccines in combination with anti-PD-1 blockade strategies have shown great promise for combination cancer immunotherapy [23]. In our study, WGP-OVA treatment was insufficient to affect PD-1 expression on T cells (Fig. S1b), which indicates that the use of such a vaccine may provide a more effective therapeutic effect when combined with anti-PD-1 therapy.

Based on the results of our experiments and previous reports, we speculated the mechanism by which oral gavage of the WGP-OVA vaccine elicited antitumor immunity responses in murine tumor models. Orally administrated WGP-OVA particles are transferred by M cells to gut-associated lymphatic tissue macrophages (GALT) [11] upon arriving in small intestinal lumen. These WGP-OVA-loading

macrophages are then migrated to secondary lymphatic organs such spleen, lymph nodes under the general circulation, where insoluble WGP are digested into small fragments and OVA antigen is processed to OVA peptides. Subsequently, active β -glucan fragments are released from macrophages to serve as an adjuvant, while OVA-peptides–MHC complex are formed on the surface of macrophages to interact with T cells for the initiation of T cell immune responses. Therefore, the WGP-based vaccine formulation not only delivered encapsulated antigen to target cells for the activation of effector T cells but also further amplified antigen immunogenicity to enhance effective tumoricidal activities.

In summary, we developed a WGP-based cancer vaccine and demonstrated that the WGP-OVA formulation not only efficiently drove M0-type BMDM polarization to the proinflammatory M1 phenotype but also offered the remarkable antigen cross-presentation for BMDMs with the assistance of the WGP vector. Orally administered WGP-OVA vaccine significantly delayed tumor progression with an increase of tumor-infiltrating OVA-specific CD8⁺ CTLs and M1 TAMs, suggesting that WGP was a potential vector for protein vaccine delivery. The effectiveness of WGP-OVA formulation here was only assessed in immunogenic tumor models; more tumor models would be needed to further verify such formulation for immunotherapy strategy.

Supplementary Information The online version contains supplementary material available at <https://doi.org/10.1007/s00262-021-03136-7>.

Acknowledgements This work was supported by grants from the National Natural Science Foundation of China (81672799 to C.Q.); Key Project of Jiangsu S &T Plan (BE2019651 to C.Q.); the Natural Science Foundation of Jiangsu Province (BK20200178 to D.J.); Changzhou Sci &Tech Program (CJ20210095 to Z.Z.) and the Youth Talent Sci &Tech Project of the Changzhou Commission of Health (QN202036 to L.H.).

Author contribution LH was involved in conceptualization, data curation, investigation, methodology, validation and writing—original draft. YB and LX contributed to data curation, methodology and resources. JP and XS performed methodology, data curation and software. ZZ and JD done methodology and resources. CQ and CT contributed to funding acquisition, supervision and writing—review and editing.

Declarations

Conflict of interest The authors declare that they have no competing interest.

References

1. Banday AH, Jeelani S, Hruby VJ (2015) Cancer vaccine adjuvants—recent clinical progress and future perspectives.

- Immunopharmacol Immunotoxicol 37(1):1–11. <https://doi.org/10.3109/08923973.2014.971963>
2. Zhang R, Billingsley MM, Mitchell MJ (2018) Biomaterials for vaccine-based cancer immunotherapy. *J Control Release* 292:256–276. <https://doi.org/10.1016/j.jconrel.2018.10.008>
 3. Deng C, Hu Z, Fu H, Hu M, Xu X, Chen J (2012) Chemical analysis and antioxidant activity in vitro of a beta-D-glucan isolated from *Dictyophora indusiata*. *Int J Biol Macromol* 51(1–2):70–75. <https://doi.org/10.1016/j.ijbiomac.2012.05.001>
 4. Qi C, Cai Y, Gunn L, Ding C, Li B, Kloecker G et al (2011) Differential pathways regulating innate and adaptive antitumor immune responses by particulate and soluble yeast-derived beta-glucans. *Blood* 117(25):6825–6836. <https://doi.org/10.1182/blood-2011-02-339812>
 5. Ensley HE, Tobias B, Pretus HA, McNamee RB, Jones EL, Browder IW et al (1994) NMR spectral analysis of a water-insoluble (1→3)-beta-D-glucan isolated from *Saccharomyces cerevisiae*. *Carbohydr Res* 258:307–311. [https://doi.org/10.1016/0008-6215\(94\)84098-9](https://doi.org/10.1016/0008-6215(94)84098-9)
 6. Plato A, Willment JA, Brown GD (2013) C-type lectin-like receptors of the dectin-1 cluster: ligands and signaling pathways. *Int Rev Immunol* 32(2):134–156. <https://doi.org/10.3109/08830185.2013.777065>
 7. Manabe N, Yamaguchi Y (2021) 3D Structural Insights into beta-Glucans and Their Binding Proteins. *Int J Mol Sci*. <https://doi.org/10.3390/ijms22041578>
 8. Miyamoto N, Mochizuki S, Sakurai K (2018) Designing an immunocyte-targeting delivery system by use of beta-glucan. *Vaccine* 36(1):186–189. <https://doi.org/10.1016/j.vaccine.2017.11.053>
 9. Huang H, Ostroff GR, Lee CK, Specht CA, Levitz SM (2013) Characterization and optimization of the glucan particle-based vaccine platform. *Clin Vaccine Immunol* 20(10):1585–1591. <https://doi.org/10.1128/CVI.00463-13>
 10. Soto ER, Ostroff GR (2008) Characterization of multilayered nanoparticles encapsulated in yeast cell wall particles for DNA delivery. *Bioconjug Chem* 19(4):840–848. <https://doi.org/10.1021/bc700329p>
 11. Aouadi M, Tesz GJ, Nicoloso SM, Wang M, Chouinard M, Soto E et al (2009) Orally delivered siRNA targeting macrophage Map4k4 suppresses systemic inflammation. *Nature* 458(7242):1180–1184. <https://doi.org/10.1038/nature07774>
 12. Tesz GJ, Aouadi M, Prot M, Nicoloso SM, Boutet E, Amano SU et al (2011) Glucan particles for selective delivery of siRNA to phagocytic cells in mice. *Biochem J* 436(2):351–362. <https://doi.org/10.1042/BJ20110352>
 13. De Marco CE, Calder PC, Roche HM (2021) beta-1,3/1,6-Glucans and Immunity: State of the Art and Future Directions. *Mol Nutr Food Res* 65(1):e1901071. <https://doi.org/10.1002/mnfr.201901071>
 14. Vetricka V, Vannucci L, Sima P (2020) beta-glucan as a new tool in vaccine development. *Scand J Immunol* 91(2):e12833. <https://doi.org/10.1111/sji.12833>
 15. Stier H, Ebbeskotte V, Gruenwald J (2014) Immune-modulatory effects of dietary Yeast Beta-1,3/1,6-D-glucan. *Nutr J* 13:38. <https://doi.org/10.1186/1475-2891-13-38>
 16. Zhang M, Kim JA, Huang AY (2018) Optimizing Tumor Microenvironment for Cancer Immunotherapy: beta-Glucan-Based Nanoparticles. *Front Immunol* 9:341. <https://doi.org/10.3389/fimmu.2018.00341>
 17. Li B, Cramer D, Wagner S, Hansen R, King C, Kakar S et al (2007) Yeast glucan particles activate murine resident macrophages to secrete proinflammatory cytokines via MyD88- and Syk kinase-dependent pathways. *Clin Immunol* 124(2):170–181. <https://doi.org/10.1016/j.clim.2007.05.002>
 18. Ning Y, Xu D, Zhang X, Bai Y, Ding J, Feng T et al (2016) beta-glucan restores tumor-educated dendritic cell maturation to enhance antitumor immune responses. *Int J Cancer* 138(11):2713–2723. <https://doi.org/10.1002/ijc.30002>
 19. Huang H, Ostroff GR, Lee CK, Specht CA, Levitz SM (2010) Robust stimulation of humoral and cellular immune responses following vaccination with antigen-loaded beta-glucan particles. *mBio*. <https://doi.org/10.1128/mBio.00164-10>
 20. Hong F, Yan J, Baran JT, Allendorf DJ, Hansen RD, Ostroff GR et al (2004) Mechanism by which orally administered beta-1,3-glucans enhance the tumoricidal activity of antitumor monoclonal antibodies in murine tumor models. *J Immunol* 173(2):797–806. <https://doi.org/10.4049/jimmunol.173.2.797>
 21. Yunna C, Mengru H, Lei W, Weidong C (2020) Macrophage M1/M2 polarization. *Eur J Pharmacol* 877:173090. <https://doi.org/10.1016/j.ejphar.2020.173090>
 22. Joffre OP, Segura E, Savina A, Amigorena S (2012) Cross-presentation by dendritic cells. *Nat Rev Immunol* 12(8):557–569. <https://doi.org/10.1038/nri3254>
 23. Xu J, Wang H, Xu L, Chao Y, Wang C, Han X et al (2019) Nanovaccine based on a protein-delivering dendrimer for effective antigen cross-presentation and cancer immunotherapy. *Biomaterials* 207:1–9. <https://doi.org/10.1016/j.biomaterials.2019.03.037>
 24. Waldman AD, Fritz JM, Lenardo MJ (2020) A guide to cancer immunotherapy: from T cell basic science to clinical practice. *Nat Rev Immunol* 20(11):651–668. <https://doi.org/10.1038/s41577-020-0306-5>
 25. Kaech SM, Wherry EJ, Ahmed R (2002) Effector and memory T-cell differentiation: implications for vaccine development. *Nat Rev Immunol* 2(4):251–262. <https://doi.org/10.1038/nri778>
 26. Warriar VU, Makandar AI, Garg M, Sethi G, Kant R, Pal JK et al (2019) Engineering anti-cancer nanovaccine based on antigen cross-presentation. *Biosci Rep*. <https://doi.org/10.1042/BSR20193220>
 27. Galluzzi L, Chan TA, Kroemer G, Wolchok JD, Lopez-Soto A (2018) The hallmarks of successful anticancer immunotherapy. *Sci Transl Med*. <https://doi.org/10.1126/scitranslmed.aat7807>
 28. Nobuoka D, Yoshikawa T, Takahashi M, Iwama T, Horie K, Shimomura M et al (2013) Intratumoral peptide injection enhances tumor cell antigenicity recognized by cytotoxic T lymphocytes: a potential option for improvement in antigen-specific cancer immunotherapy. *Cancer Immunol Immunother* 62(4):639–652. <https://doi.org/10.1007/s00262-012-1366-6>
 29. Park YM, Lee SJ, Kim YS, Lee MH, Cha GS, Jung ID et al (2013) Nanoparticle-based vaccine delivery for cancer immunotherapy. *Immune Netw* 13(5):177–183. <https://doi.org/10.4110/in.2013.13.5.177>
 30. Belfiore L, Saunders DN, Ranson M, Thurecht KJ, Storm G, Vine KL (2018) Towards clinical translation of ligand-functionalized liposomes in targeted cancer therapy: Challenges and opportunities. *J Control Release* 277:1–13. <https://doi.org/10.1016/j.jconrel.2018.02.040>
 31. Chesson CB, Huante M, Nusbaum RJ, Walker AG, Clover TM, Chinnaswamy J et al (2018) Nanoscale Peptide Self-assemblies Boost BCG-primed Cellular Immunity Against Mycobacterium tuberculosis. *Sci Rep* 8(1):12519. <https://doi.org/10.1038/s41598-018-31089-y>
 32. Liu M, Luo F, Ding C, Albeituni S, Hu X, Ma Y et al (2015) Dectin-1 Activation by a Natural Product beta-Glucan Converts Immunosuppressive Macrophages into an M1-like Phenotype. *J Immunol* 195(10):5055–5065. <https://doi.org/10.4049/jimmunol.1501158>
 33. Kumar R, Kumar P (2019) Yeast-based vaccines: New perspective in vaccine development and application. *FEMS Yeast Res*. <https://doi.org/10.1093/femsyr/foz007>

34. Melssen M, Slingluff CL Jr (2017) Vaccines targeting helper T cells for cancer immunotherapy. *Curr Opin Immunol* 47:85–92. <https://doi.org/10.1016/j.coi.2017.07.004>
35. Xie Y, Akpınarlı A, Maris C, Hipkiss EL, Lane M, Kwon EK et al (2010) Naive tumor-specific CD4(+) T cells differentiated in vivo eradicate established melanoma. *J Exp Med* 207(3):651–667. <https://doi.org/10.1084/jem.20091921>
36. Quezada SA, Simpson TR, Peggs KS, Merghoub T, Vider J, Fan X et al (2010) Tumor-reactive CD4(+) T cells develop cytotoxic activity and eradicate large established melanoma after transfer into lymphopenic hosts. *J Exp Med* 207(3):637–650. <https://doi.org/10.1084/jem.20091918>
37. Ahrends T, Babala N, Xiao Y, Yagita H, van Eenennaam H, Borst J (2016) CD27 Agonism Plus PD-1 Blockade Recapitulates CD4+ T-cell Help in Therapeutic Anticancer Vaccination. *Cancer Res* 76(10):2921–2931. <https://doi.org/10.1158/0008-5472.CAN-15-3130>
38. Hassan SB, Sorensen JF, Olsen BN, Pedersen AE (2014) Anti-CD40-mediated cancer immunotherapy: an update of recent and ongoing clinical trials. *Immunopharmacol Immunotoxicol* 36(2):96–104. <https://doi.org/10.3109/08923973.2014.890626>
39. Peng W, Liu C, Xu C, Lou Y, Chen J, Yang Y et al (2012) PD-1 blockade enhances T-cell migration to tumors by elevating IFN-gamma inducible chemokines. *Cancer Res* 72(20):5209–5218. <https://doi.org/10.1158/0008-5472.CAN-12-1187>
40. Kim HJ, Cantor H (2014) CD4 T-cell subsets and tumor immunity: the helpful and the not-so-helpful. *Cancer Immunol Res* 2(2):91–98. <https://doi.org/10.1158/2326-6066.CIR-13-0216>
41. Li B, Cai Y, Qi C, Hansen R, Ding C, Mitchell TC et al (2010) Orally administered particulate beta-glucan modulates tumor-capturing dendritic cells and improves antitumor T-cell responses in cancer. *Clin Cancer Res* 16(21):5153–5164. <https://doi.org/10.1158/1078-0432.CCR-10-0820>
42. Drovok M, Davydova Y, Popova N, Kapranov N, Starikova O, Mikhaltsova E et al (2020) High expression of granzyme B in conventional CD4+ T cells is associated with increased relapses after allogeneic stem cells transplantation in patients with hematological malignancies. *Transpl Immunol*. <https://doi.org/10.1016/j.trim.2020.101295>
43. Geller A, Shrestha R, Yan J (2019) Yeast-Derived beta-Glucan in Cancer: Novel Uses of a Traditional Therapeutic. *Int J Mol Sci*. <https://doi.org/10.3390/ijms20153618>
44. Zheng B, Ren T, Huang Y, Sun K, Wang S, Bao X et al (2018) PD-1 axis expression in musculoskeletal tumors and antitumor effect of nivolumab in osteosarcoma model of humanized mouse. *J Hematol Oncol* 11(1):16. <https://doi.org/10.1186/s13045-018-0560-1>
45. Yu X, Gao R, Li Y, Zeng C (2020) Regulation of PD-1 in T cells for cancer immunotherapy. *Eur J Pharmacol* 881:173240. <https://doi.org/10.1016/j.ejphar.2020.173240>

Publisher's Note Springer Nature remains neutral with regard to jurisdictional claims in published maps and institutional affiliations.